DEVELOPMENT OF FIELD IONIZATION FOR THE IMPROVEMENT OF MASS SPECTROMETRY

by

Paul J. Bryant
James M. Phillips

INTERIM SCIENTIFIC REPORT
25 March 1968 - 25 March 1969

NASA Contract No. NAS 12-646

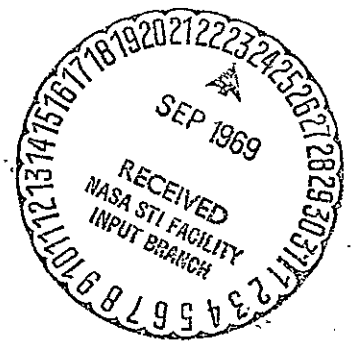

For

Dr. Wayne L. Lees, KIA
National Aeronautics and Space Administration
Electronics Research Center
575 Technology Square
Cambridge, Massachusetts 02139

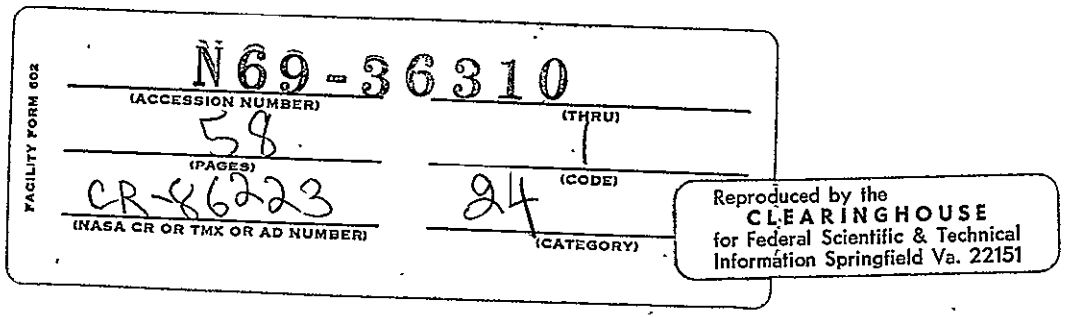

PREFACE

The subject matter of this research program includes the proper description and interpretation of field ionization data, the improvement of ionizer designs, and the adaptations to mass spectrometry. The program is sponsored by the National Aeronautics and Space Administration, Electronics Research Center, Boston, Massachusetts. Dr. Wayne L. Lees is the project monitor for NASA-ERC. Mr. Paul R. Yeager of the NASA Langley Research Center is also providing monitoring services.

This interim scientific report covers the work performed in the first year of the program, 25 March 1968 through 25 March 1969. The work has been performed in the Physics Department, University of Missouri - Kansas City. Dr. Paul J. Bryant and Dr. James M. Phillips serve as principal investigators and authors of this report. They were assisted during this report period by Mr. Paul L. Gutshall, Mr. G. David Moore, and Mr. Charles Gosselin, staff members; Mr. Dale Holt, Miss Carol Stephenson and Mr. George Mansell, graduate research assistants.

Communications and suggestions regarding this research program will be sincerely appreciated.

TABLE OF CONTENTS

List of Figures

List of Figures (Concluded)

SUMMARY

This report describes the development of an efficient field ionization ion source and quadrupole focusing system for the production of ions for mass spectrometry. The phenomena of field ionization by the quantum mechanical "tunneling" of an electron out of the potential barrier of an atom or molecule has been discussed and utilized by a number of workers.[1,2,3,6,7] The application of field ionization sources to mass spectrometry has been limited by the low ion yield as compared to other standard ionization techniques.

A new carbon filament ionizer, designed and utilized on this program, has increased ion yield by two orders of magnitude, making this technique competitive with electron impact sources. The new ionizer coupled with an ion lens system designed for focusing and retarding the high energy field ions has been successfully used as an ion source for a commercial quadrupole mass spectrometer.

The mass spectrometer resulting from the union of the commercial unit with the field ion source and lens system has several unique features. The gas sampling and spectrometer chambers are separately evacuated so that toxic and corrosive gaseous environments may be analysed without damaging or contaminating the mass spectrometer. Gases in the sampling chamber may be analyzed by either electron bombardment or field ionization and the results compared. The field ionization source and lens system has been specifically designed to reduce the possibility of a background signal due to spurious radiation such as x-rays or electrons. The sets of quadrupole lenses and immersion type lenses accomplish focusing over a long path length while reducing background affects from the ion source to negligible levels.

Thus, the high ion yield obtained with the new type field ion sources, and the preliminary results with the mass spectrometer show the feasibility of practical applications.

In addition to the experimental results, ion yields have been computed from the transmission probabilities for an electron to pass through a molecular potential barrier. Transmission probabilities were calculated by two methods, the WKB method, and a direct solution of the linear Schrödinger equation. Both of these methods have been programed for the computer so that a direct comparison between experiment

and theory is possible by inserting the experimental parameters into the computer programs. The results of a third calculation of the transmission probability for the intermediate field range predicts an increase of ion yield of two orders of magnitude for a gain in field strength of 1 V/Å.

The results of these calculations will serve as a guide to optimization of ion yield in a working mass spectrometer.

DEVELOPMENT OF FIELD IONIZATION FOR THE IMPROVEMENT OF MASS SPECTROMETRY

by

Paul J. Bryant
James M. Phillips

INTERIM SCIENTIFIC REPORT
25 March 1968 - 25 March 1969

NASA Contract No. NAS 12-646

I. INTRODUCTION

The build-up of toxic trace contaminants in a cabin atmosphere poses a serious problem for long term operation. The use of a mass spectrometer employing an electron impact ionization source for monitoring the build up of these trace contaminants has several disadvantages: 1) the cracking patterns complicate the analysis of the atmosphere; 2) in many cases parent molecules are eliminated by electron impact; and 3) the telemetering and monitoring of such data is complicated by the large number of signals and the multiple contributions to individual signals.

The use of a field ion source for mass spectrometry provides solutions to the problems presented above. The electron tunneling process in field ionization may occur with the least amount of energy input to a molecule; thus fragmentation and the resulting complexity of the mass spectra are minimized. The parent molecule generally yields the only significant, or at least the most intense peak of the mass spectra. The reduction in "cracking" and the intensity of the parent peaks minimizes the problems of telemetering and monitoring mass spectrometer data.

The low yield of typical field ion sources (tips and wires), as compared to electron impact sources, has limited their usefulness in mass spectrometry. The purpose of the research to be described in this report is the development of a field ionization source with improved ion yield for application to mass spectrometry.

The purpose of the theoretical calculations is to provide support of the experimental effort and to develop a more fundamental description of the basic physical mechanism of field ionization. These goals are achieved by a study of the kinetics of the molecular interactions with the emitter geometry and a quantum mechanical theory of the ionization rates. The methods employed have included: the WKB Solution of Schrödinger's equation for bound electrons in the potential well of a molecule in a high electric field; and band theory considerations for the ionizer material.

II. EQUIPMENT AND RESULTS

The experimental portion of the program is presented in two sections; (A) ion yield measurements and (B) mass spectrometry. The experimental procedures and results for the ion yield measurements are presented in Section A. The

design, construction, and testing of special equipment necessary for the adaptation of the field ion source to mass spectrometry is discussed in Section B.

A. ION YIELD

The total ion production from several experimental ionizers was measured with special equipment (see section 1) under known conditions. The data is presented in section 2 below in comparison with other ionizer designs.

1. Equipment

The equipment required for the ion yield measurements includes: (a) a field ion microscope tube, (b) a gas control system, and (c) an evacuation system. The overall system used for these measurements, along with a quadrupole mass spectrometer, is shown in Fig. 1.

a. Field Ionization Tube

A special field ion microscope tube was designed and constructed for the measurement of total ion yield. Total ion yield values for given values of gas supply function and field strength are necessary for the interpretation of field ion data. Thus a spherical tube with a collector which completely surrounds the ionizer structure was employed (see Fig. 1).

The tube may be readily disassembled for mounting various experimental ionizer structures. Electrical vacuum feedthroughs are provided for the high voltage ionizer, and the ion collector. An electrical guard ring is also provided to prevent current flow from the collector structure to the high voltage electrode. A re-entrant glass feedthrough provides a long path for up to 30 KV insulation. An optically transparent stannous oxide coating on the inner glass bulb wall constitutes the ion collector. A Keithley model 610B electrometer is employed for ion current measurements.

b. Gas Control System

The gas control system consists of the gas inlet unit and the pressure measurement system.

The gas inlet system employs a variable micrometer leak valve, connected with stainless steel tubing to a commercial

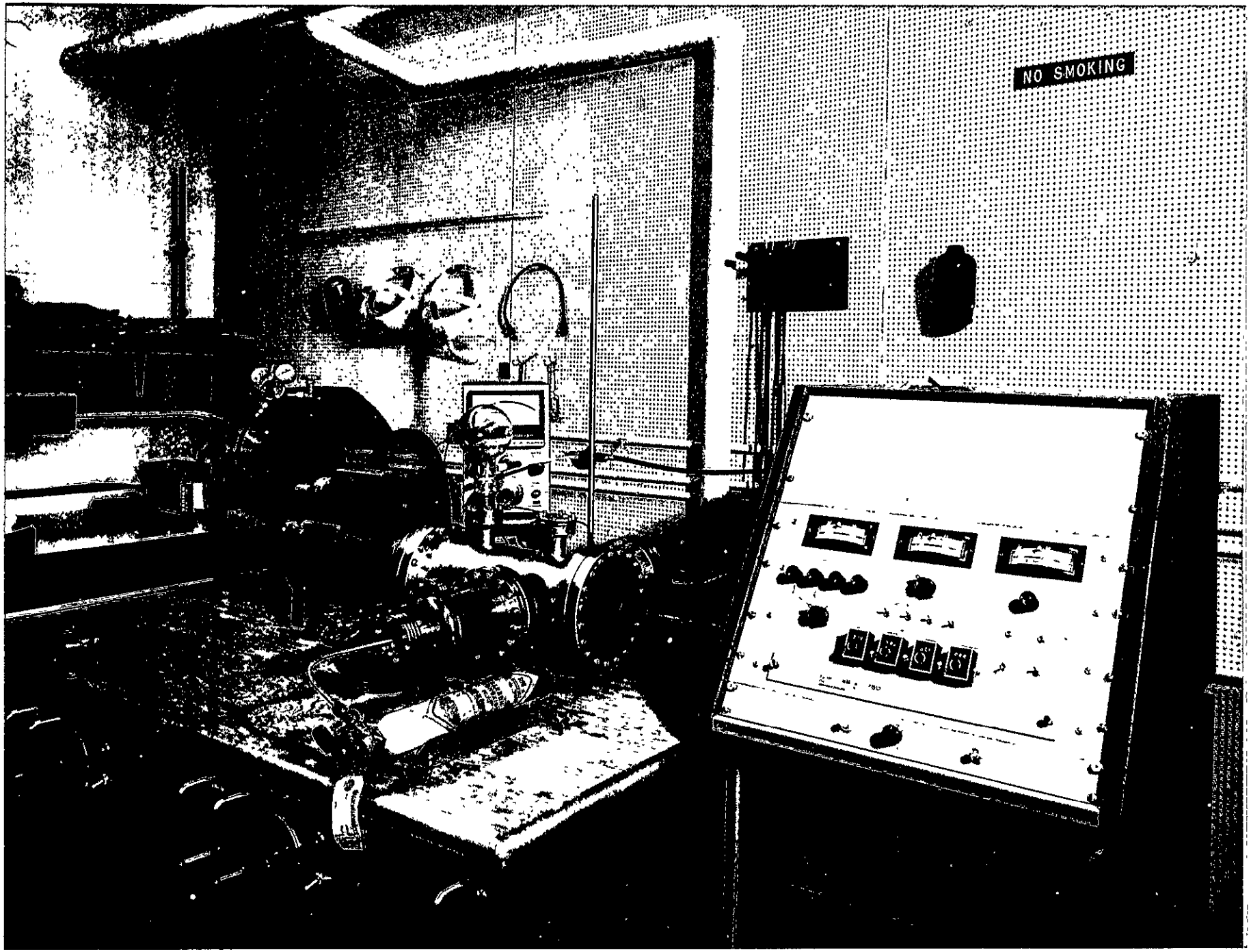

Fig. 1. Experimental apparatus used to measure total ion yield from various field ionizers.

vacuum flange. High purity gases from lecture bottles are admitted through the variable leak valve. A dynamic equilibrium is established within the system by adjusting the micrometer valve until the desired pressure is maintained between the inlet flow and the evacuation rate.

The second part of the gas control system is a dual range pressure measurement unit. A Granville-Phillips ionization and thermionic gauge control unit is employed in conjunction with a Varian model UHV-12 gauge tube. Pressure measurements from 10 Torr to 10^{-11} Torr may be made with corrections for x-ray photo-current at the lower values. Accurate pressure values are needed to determine the gas molecule supply function for field ionization.

c. Evacuation System

Several different pumping mechanisms are employed for various stages of the evacuation process. A mechanical fore pump and fluid diffusion pump are used for initial evacuation and during the period of bake-out of the remaining system. Getter-ion and titanium sublimation pumps are available for ultra-high vacuum operation.

The diffusion pump unit is necessary when an inert gas such as helium is being used as the working fluid since the getter-ion pump is not capable of handling large quanities of inert gases. A special chemical trap is employed to prevent diffusion pump fluid from back-streaming into the system. A new artificial fluid (Santovac 5) compound is being used. A large volume titanium sublimation pump is also included in the system.

A differential evacuation capability has been provided so that the gas ionization chamber may be exposed to some environment of interest while the main body of the mass spectrometer is maintained in ultra high vacuum. The diffusion pump system may evacuate the ionization chamber while the getter-ion-sublimation pump system operates on the mass spectrometer chamber. Thus, many different gas environments including inert and corrosive gases may be analyzed while the mass spectrometer is maintained clean under high vacuum.

2. Field Ionization Yield Data

The total ion current yield characteristics have been studied for experimental field ionizers. Ion current versus voltage data from four different ionizers are presented in

Table I. The ions were formed from trace amounts of the toxic gas carbon monoxide. Comparative data for equivalent conditions is also shown in Table I. The data normalized to unit gas pressure and unit length of the extended ionizers. That is, a comparison of data is presented for the number of gas ions formed from an equivalent number of neutral molecules and from an equal ionizer length. Thus the data of Table I may be used to determine the actual ion current in amps which can be provided to any instrument by multiplying the appropriate ion acceptance aperature dimension and transmission value, and the gas pressure by the yield value given in amps/Torr-mm.

The ion yield values obtained from four of the experimental ionizers tested under this research program are listed under the heading, "filament." The highest yield values found in the scientific literature are reported by Robertson and Viney[2] using a 10 micron diameter platinum wire with CO gas and are listed for various voltages under the heading, "wire." The ion yield values obtained under this research program with approximately 1 micron diameter carbon filaments are from 10^2 to 10^3 times higher than the best values reported for a wire. In addition, the wire data is about 10^2 times greater than values reported for a metal tip. Thus the ion yield obtained with the experimental filament ionizers developed under this program is sufficient for practical applications to the operation of instruments such as mass spectrometers.

The experimental equipment employed for the ion yield measurements is shown in Fig. 1. Trace quantities of carbon monoxide were admitted from a lecture bottle, as seen in Fig. 1. The spherical field ion microscope bulb collects the ion current generated by the experimental ionizers. The electrometer shown is connected by a short length of co-axial cable to the field ion bulb. The bulb is shown exposed in Fig. 1 but during operation it is enclosed in a Faraday cage for electrostatic shielding. With this experimental apparatus an ionizer filament and holder assembly has been developed for use in a mass spectrometer.

Expressions relating the ion current yield to the electric field, emitter geometry, emitter and gas temperature, emitter material and the species of gas molecules are presented below for both the high and the low field cases. The details of the derivation of these equations are presented in Appendix I (pp. 26-31).

Voltage	Ion Current Yield (amp/torr-mm)	
	Wire[1/]	Filament
8000	----------	(1) 1.4×10^{-5} (2) 5.3×10^{-5} (3) 4.7×10^{-6} (4) 4.2×10^{-5}
13000	8.3×10^{-8}	(1) 9.2×10^{-5} (2) 1.4×10^{-4} (4) 2.0×10^{-4}
16000	5.2×10^{-7}	(1) 1.2×10^{-4} (4) 3.8×10^{-4}

Table I. Response data for the carbon filaments of this program compared to the platinum wires of Ref. 1; the data is normalized for gas pressure and unit length of the ionizer.

For the high field case the total ion current is

$$i = q2\pi R_o \sigma_c^{\frac{1}{2}} Lp(2\pi mkT)^{-\frac{1}{2}}$$

For low fields

$$i \simeq 2\pi LC_g \tau^{-1} qR_o \left(\frac{T_g}{T_t}\right)^{\frac{1}{2}} \exp\left(-V(F_o)/kT_g\right) X_c$$

Figure 2 shows the relative number of ions formed at a distance X from the emitter surface for low, intermediate and high fields.

The total ion current is dependent on the transmission probabilities of electrons through the potential barrier of the molecule. Transmission probabilities were calculated by both the WKB method and a direct solution to the Schrödinger equation. The details of these calculations are presented in Appendix II (pp. 32-37).

The potential function used in the WKB approximation is presented in Figure 3. The transmission probabilities calculated by the WKB method are presented graphically in Figure 4 and in Table II as a function of the energy deficit of the ion, E_d.

The potential function used for the direct solution of the Schrodinger equation is presented in Figure 5. The transmission probabilities as a function of the ion energy deficit are presented in Figure 6 and in tabular form in Table III. Figure 7 and Table IV indicate the variation of the Transmission probability at the critical distance, X_c, as a function of field strength.

A comparison of the results of the two calculational methods shows that the WKB method predicts a transmission probability four orders of magnitude higher than the Schrödinger method for the same field strength values. The Schrödinger method predicts fine structure in the transmission probability which has been observed and explained by Jason[3]. The direct solution of the Schrödinger equation also indicates a change in the transmission probability of two orders of magnitude when the field strength, in the intermediate field, is varied by 1 V/Å.

Proposed improvements to the theory of field ionization, utilizing molecular orbital characterization and Band theory, are presented in Appendix III (pp. 38-50).

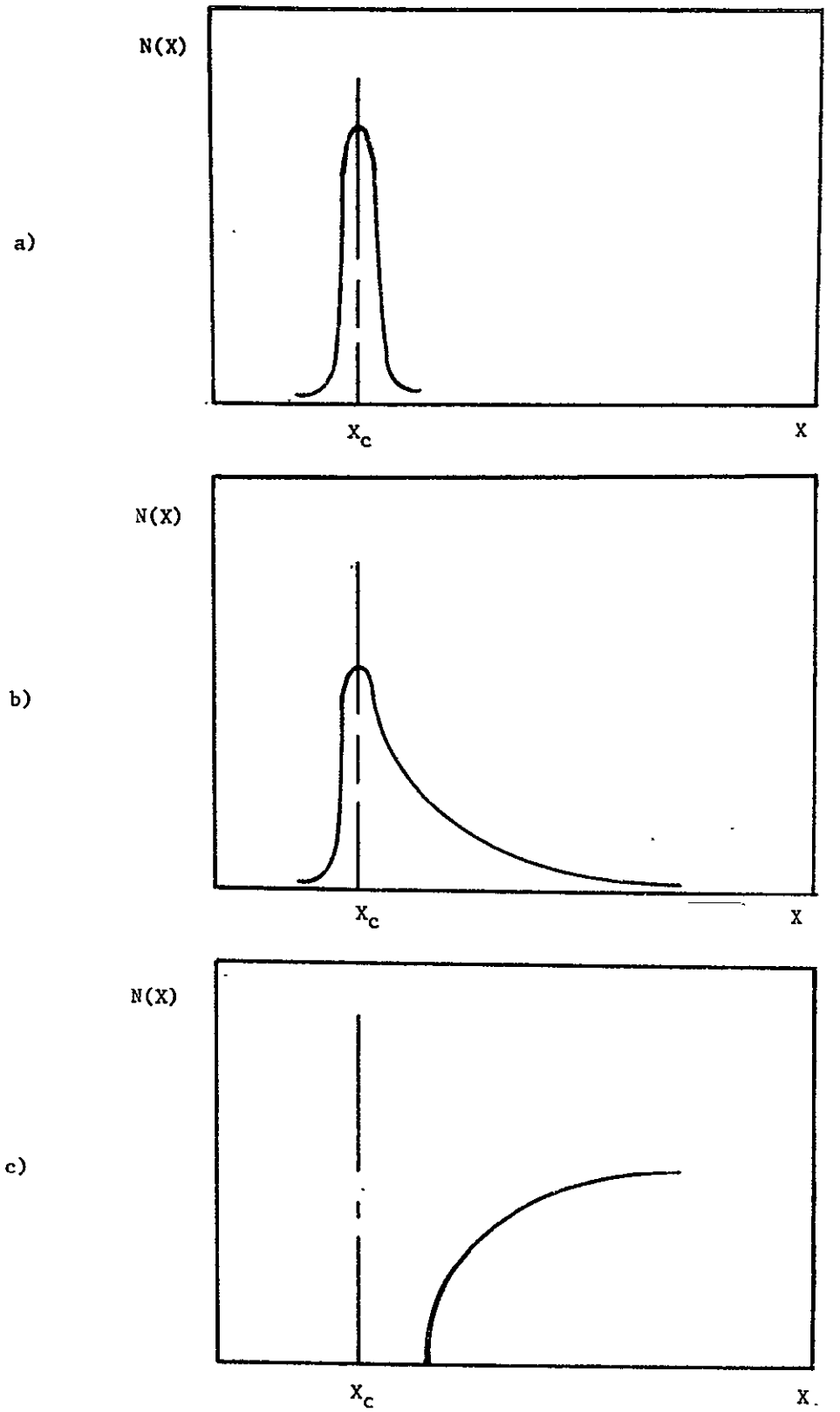

Fig. 2. Plots of the relative numbers of ions formed (N) as a function of distance (X) from the ionizer surface for the cases: (a) low field, (b) intermediate field, and (c) high field.

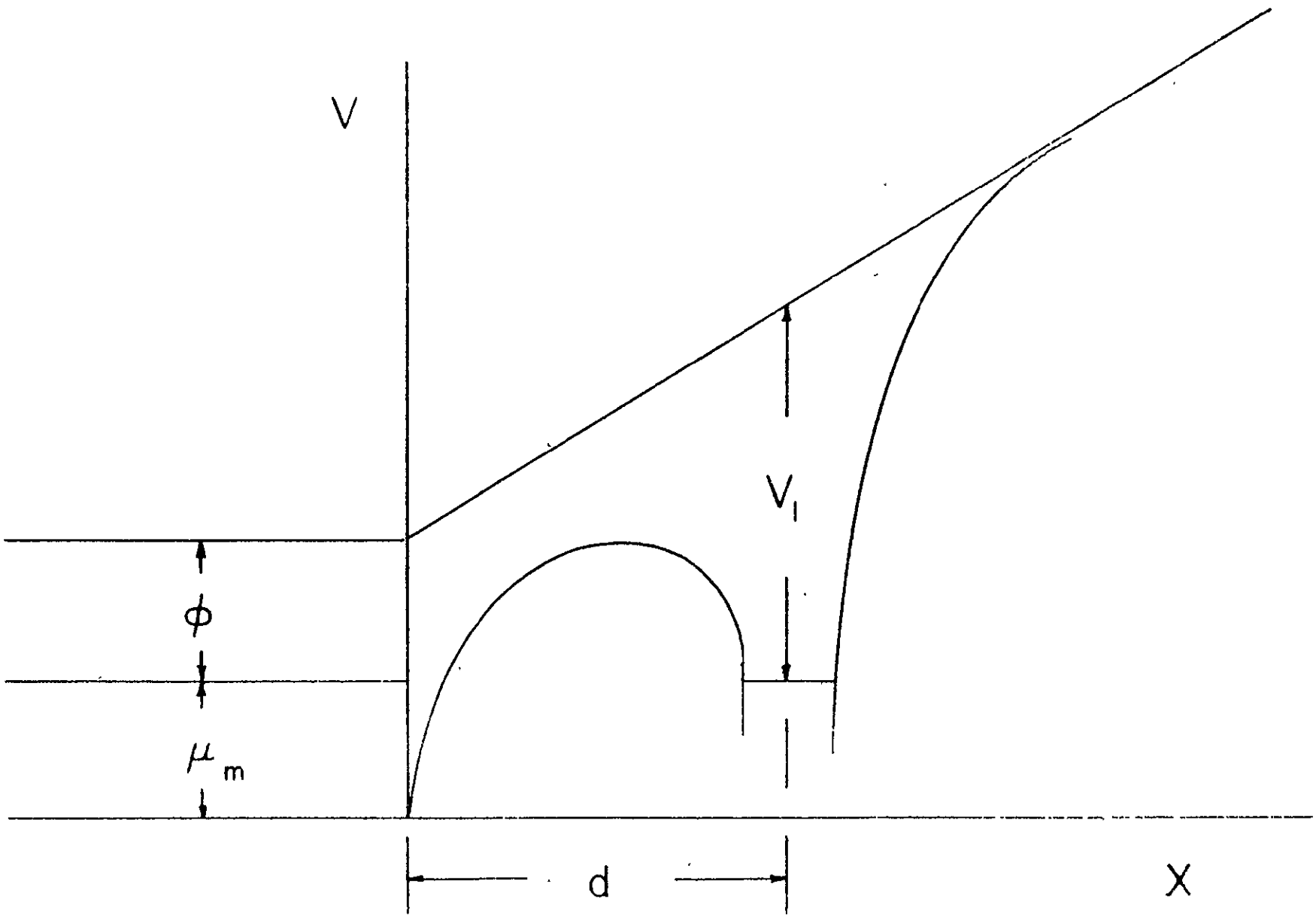

Fig. 3. A diagram of the potential energy of an electron in the presence of a molecule, a metal surface, and an electric field. This potential was used in the WKB calculation.

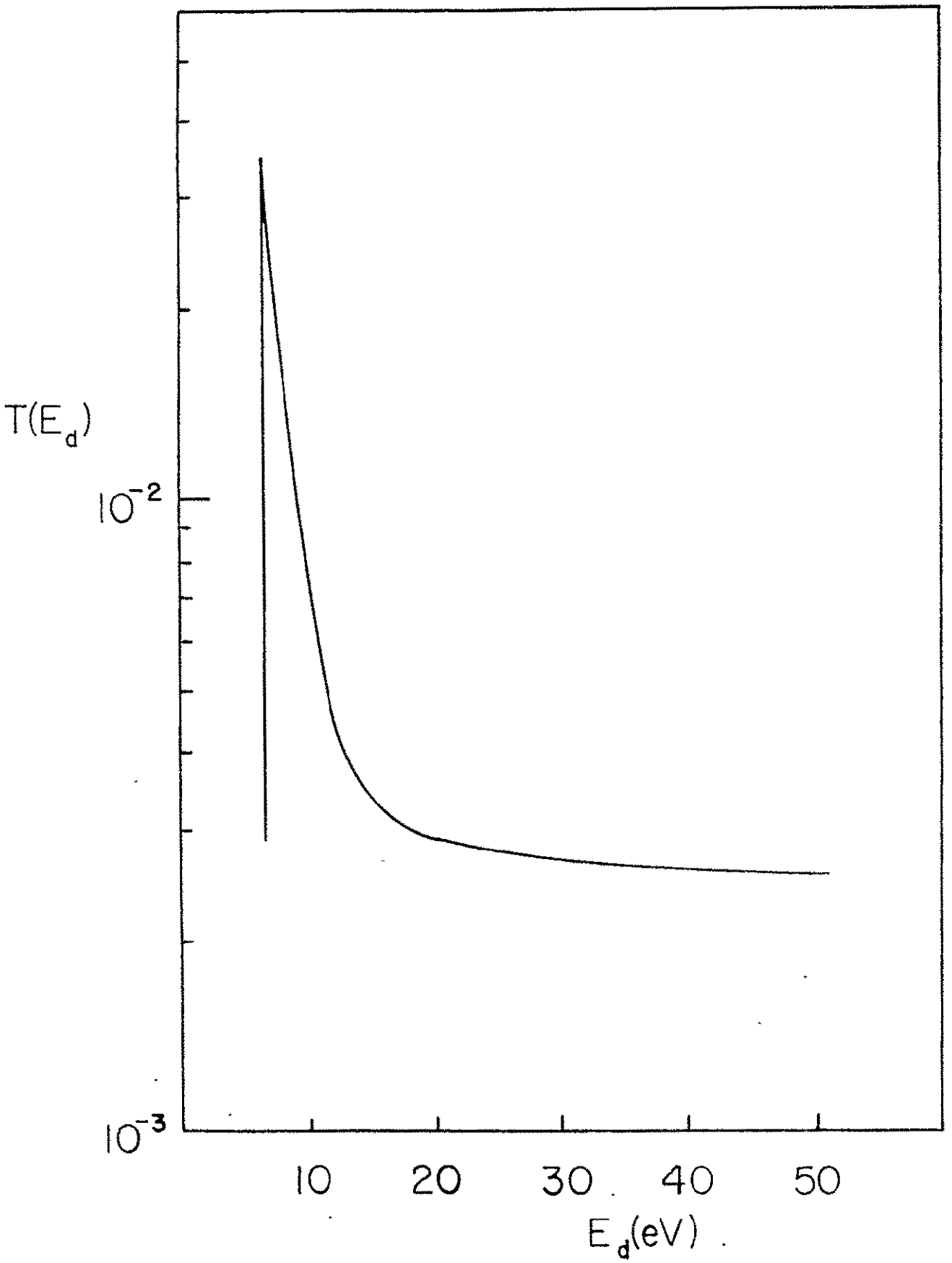

Fig. 4. A plot of the transmission probability as calculated by the WKB method.

TABLE II

TRANSMISSION PROBABILITY BY THE WKB METHOD

E_d in eV	$T(E_d)$
6.101	4.117×10^{-2}
7.250	2.148×10^{-2}
8.421	1.251×10^{-2}
9.605	8.163×10^{-3}
10.80	5.929×10^{-3}
12.00	4.713×10^{-3}
13.21	4.015×10^{-3}
14.43	3.592×10^{-3}
15.65	3.322×10^{-3}
16.87	3.143×10^{-3}
18.10	3.019×10^{-3}
19.33	2.931×10^{-3}
20.56	2.866×10^{-3}
21.79	2.817×10^{-3}
23.03	2.780×10^{-3}
24.26	2.751×10^{-3}
25.50	2.728×10^{-3}
26.74	2.709×10^{-3}
27.97	2.694×10^{-3}
29.22	2.681×10^{-3}
30.46	2.671×10^{-3}
31.70	2.662×10^{-3}
32.94	2.655×10^{-3}
34.18	2.649×10^{-3}
35.42	2.643×10^{-3}
36.67	2.639×10^{-3}
37.91	2.635×10^{-3}
39.16	2.631×10^{-3}
40.40	2.628×10^{-3}

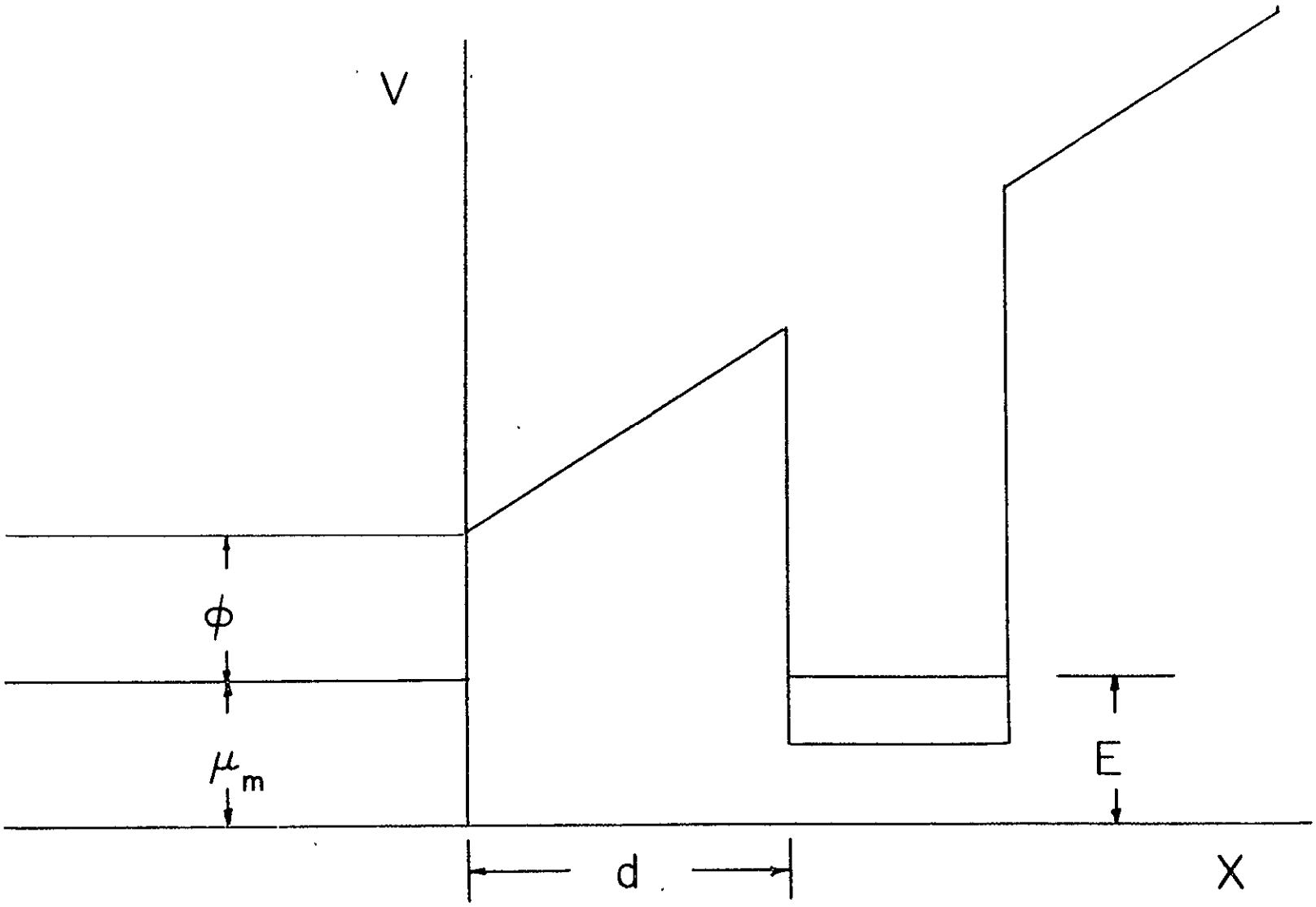

Fig. 5. The potential energy plot used in the direct solution of the linear Schrödinger equation.

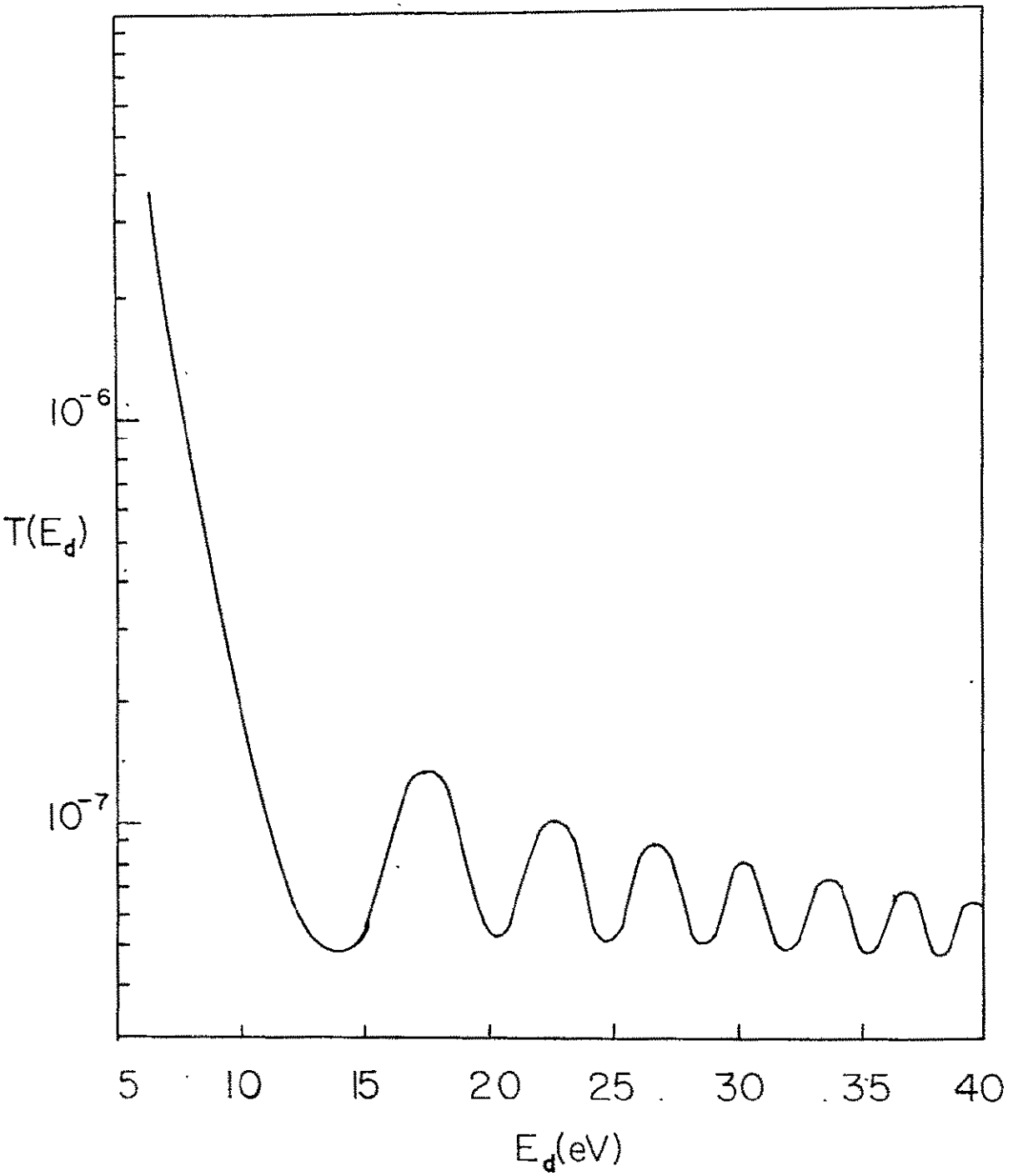

Fig. 6. The transmission probability as calculated by the direct solution of the linear Schrödinger equation.

TABLE III

TRANSMISSION PROBABILITY BY THE DIRECT SOLUTION OF THE SCHRODINGER EQUATION

E_d in eV	$T(E_d)$
6.4	3.69×10^{-6}
8.0	8.77×10^{-7}
10.0	2.03×10^{-7}
12.0	1.15×10^{-7}
14.0	4.72×10^{-8}
16.0	6.98×10^{-8}
18.0	1.25×10^{-7}
20.0	5.44×10^{-8}
22.0	8.62×10^{-8}
24.0	6.27×10^{-8}
26.0	7.09×10^{-8}
28.0	5.86×10^{-8}
30.0	7.35×10^{-8}
32.0	5.06×10^{-8}
34.0	7.12×10^{-8}
36.0	5.50×10^{-8}
38.0	5.00×10^{-8}
40.0	6.38×10^{-8}

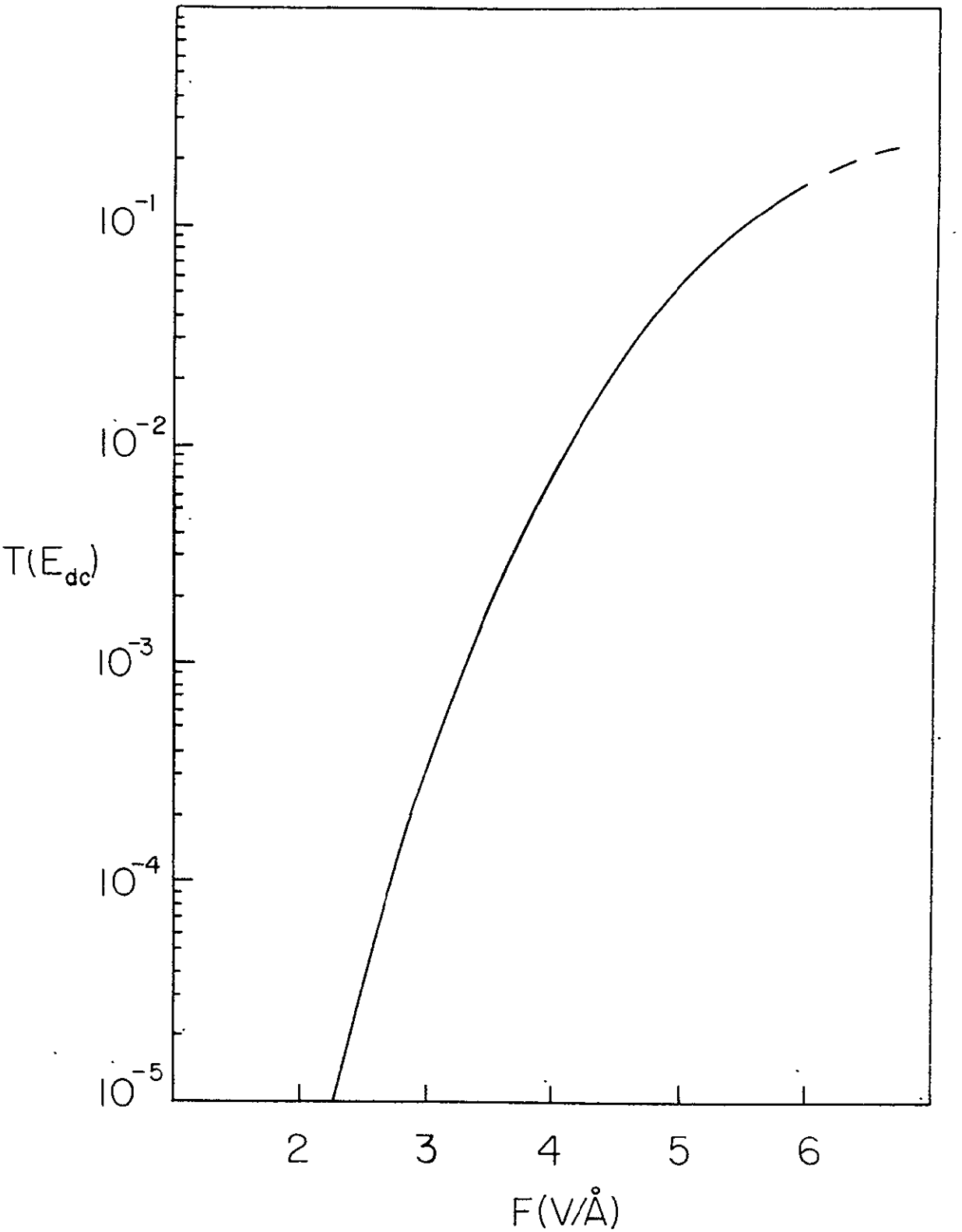

Fig. 7. Transmission probability at the critical distances for a varying electric field.

TABLE IV

TRANSMISSION PROBABILITY AT THE CRITICAL DISTANCE

Fm V/Å	$T(E_{dc})$
2.0	1.91×10^{-7}
2.2	5.70×10^{-7}
2.4	2.08×10^{-6}
2.6	6.24×10^{-6}
2.8	1.59×10^{-5}
3.0	3.60×10^{-5}
3.2	9.14×10^{-5}
3.4	1.76×10^{-4}
3.6	3.14×10^{-4}
3.8	5.28×10^{-4}
4.0	8.42×10^{-4}
4.2	1.29×10^{-3}
4.4	1.89×10^{-3}
4.6	2.68×10^{-3}
4.8	3.70×10^{-3}
5.0	4.97×10^{-3}

B. Mass Spectrometry

The special equipment required for the application of field ionization to mass spectrometry includes: (1) a field ion source and ion focusing system, (2) a mass spectrometer, (3) an evironmental sampling system, and (4) an ultra-high vacuum system. Each of these systems is described in detail below. The overall design of the system is represented schematically in Fig. 8. The field ion source and ion focusing systems are shown in detail in Figs. 8-10. The operation of the total system yielding a field ion mass spectra, is shown in Fig. 11.

1. Field Ion Source and Ion Focusing System

The purpose of this phase of the program was the generation of ions from a neutral gas and the introduction of those ions into a mass spectrometer. A small diameter wire or hemispherical tip may be used alternately[2] as an ionizer in this design. An array of quadrupole lenses and immersion lenses,[3,4,5] see Fig. 9, focus the ions into a quadrupole mass spectrometer.

The ionizer system is capable of operating with a potential difference as high as 40 kilo-volts. Thus, the desired field strength values covering low, intermediate, and high fields, from 1.5 to 3.5 volts/Angstrom, may be achieved with a wide range of emitter sizes. A high potential gradient is maintained between the ionizer and the first acceleration aperture. The geometry is arranged so that a large fraction of the field lines from the ionizer are directed toward this first aperture. Thus a high percentage of the ions should pass through the large 2.54 cm diameter acceleration aperture.

Ions generated in the high electric field gain from 10 to 30 KeV of kinetic energy in passing from the ionizer to the potential of the accelerating aperture. (Their energy may be retarded to a few KeV by an intermediate lens.) X-rays and other spurious radiation may be generated. Thus three problems must be handled: focusing of high energy ions; retardation of their energy before mass spectrometer analysis; and reduction of the incoherent background. The system of high voltage double quadrupole and immersion type lenses shown in Figs. 8 and 9 is designed to focus the high energy ions onto a small exit aperture. Since this aperture subtends an angle of only 1/3 of a degree from the source, incoherent background signals are substantially reduced. That is, the combination of a long path length and a small final aperture reduces the background of spurious signals reaching the mass spectrometer.

The final stage of the lens system consists of a field retardation unit designed to minimize the natural defocusing effect. The final energy of the ions must be reduced to less than 100 eV for proper analysis by the quadrupole mass

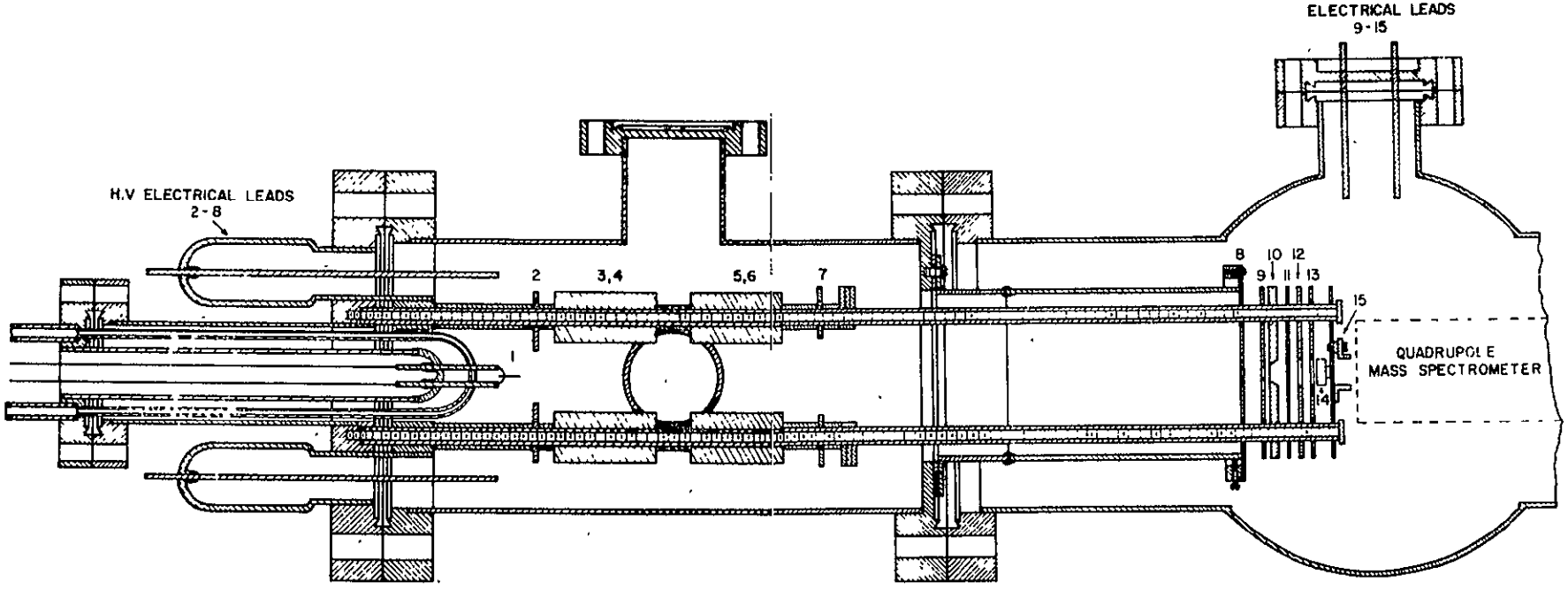

Fig. 8. Ion lens assembly, from left to right,: gas inlet, field ionizer and ion focusing sub-systems to supply field generated ions for mass spectrometry.

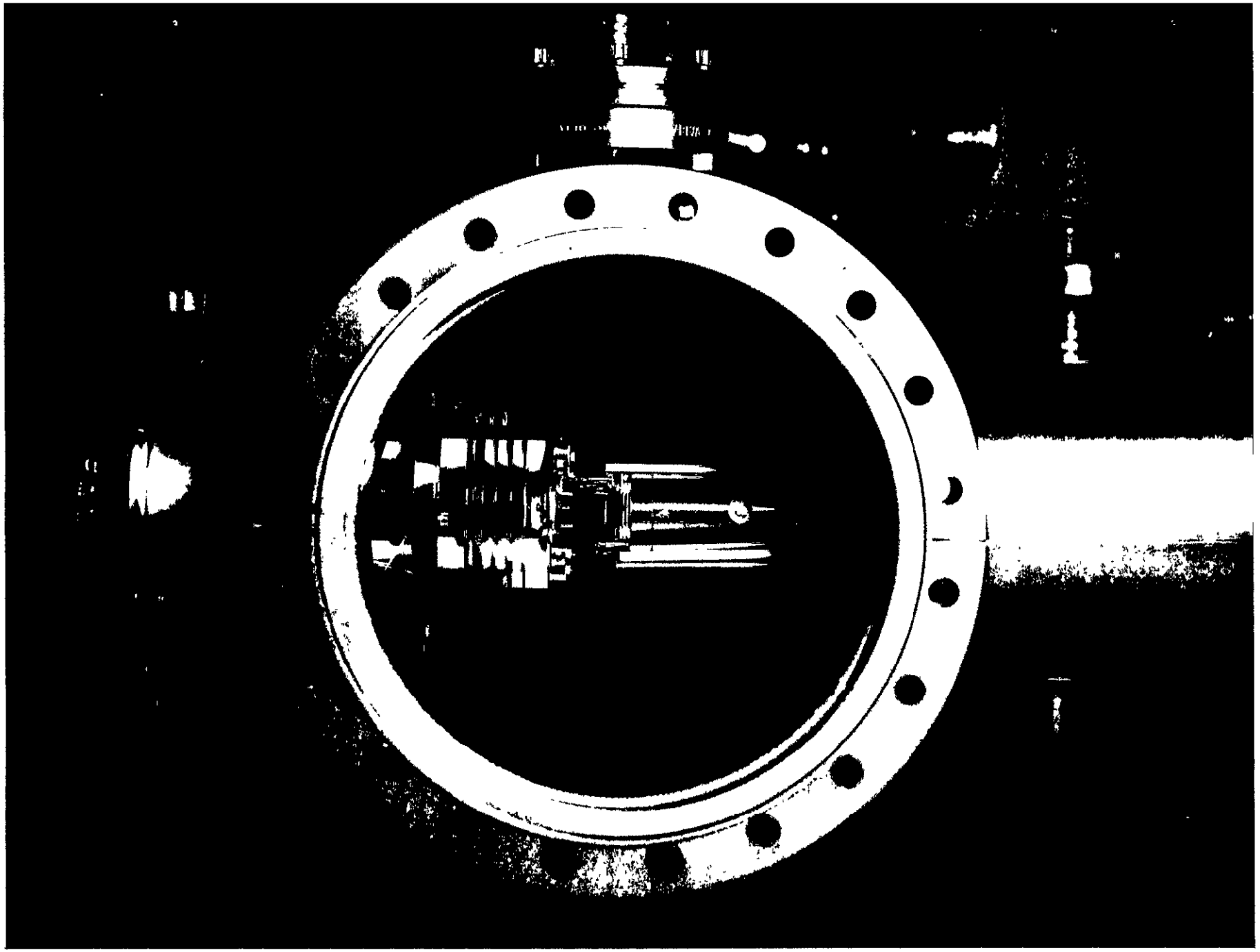

Fig. 9 Interior view of vacuum system showing the field ion lens, left and quadrupole mass spectrometer, right.

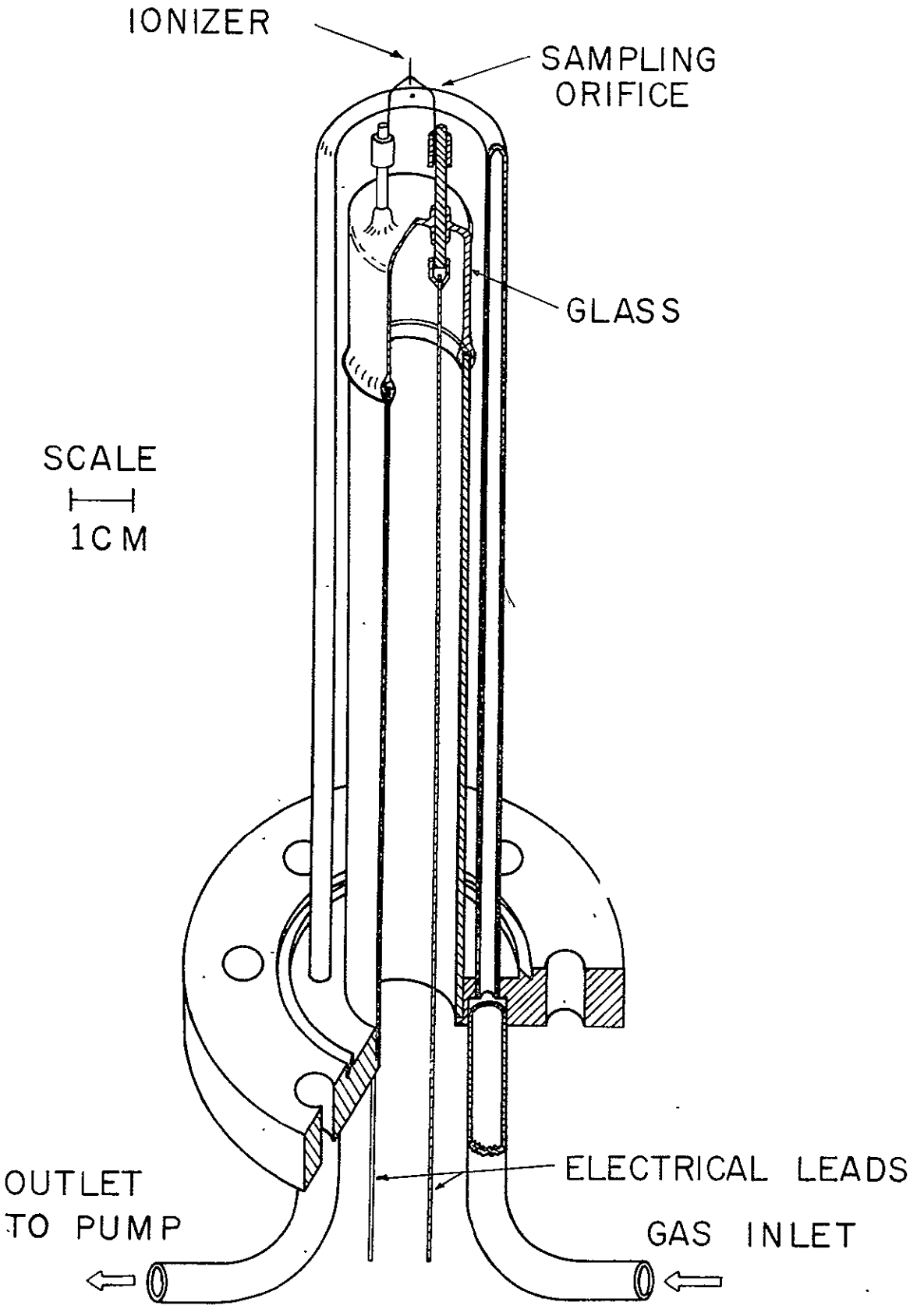

Fig. 10. A gas inlet system and field ionizer for direct sampling of high pressure atmospheres.

spectrometer. The retarding lens system employs a 3.2 mm thick disc with a 40 mesh per cm nickel screen on both faces. This grid screen has a transmission value for ions of 68% thus permitting a significant fraction of the ions to pass through the retarding plane.

The retarding field acts as a repeller for ions approaching the retarding plane thus a defocusing of the beam occurs. An additional electrode has been placed in front of the retarding lens to provide a focusing field for the decelerating ions. Following the retarding plane a unipotential lens is used to focus the ions through a set of x and y deflection electrodes onto the entrance aperture of the quadrupole mass spectrometer.

2. The Mass Spectrometer

Ions produced by means of "high" or "intermediate" fields (from 2×10^8 to 5×10^8 v/cm) are found to possess an energy spread of approximately 30 eV. Ions generated by means of a "Low" field ($1 - 2 \times 10^8$ v/cm) may be essentially mono-energetic. An ionization source for mass spectrometry of gas molecules generally requires the use of intermediate or high fields to avoid the complications which occur from gas molecule interactions with the ionizer surface at low field. Therefore, the spectrum of ion energies must be tolerated if the complications inherent in low field operation are to be avoided. This energy spread will not preclude good resolution by a quadrupole mass filter type spectrometer which is relatively insensitive to energy.

The spectrometer selected for this study filters the ions according to their mass rather than their momentum. This feature is particularly applicable for the analysis of field ionized molecules which have a fixed mass but varying momentum values. The original design of such an instrument was called a mass filter. That is, an instrument which filters selected ions in the region between four equi-spaced rods or poles. Thus, the term quadrupole was adopted to describe such instruments.

The commercial unit, purchased by the University of Missouri for this program, is a Spectra Scan 750 constructed by Finnigan Instruments and distributed by the Granville-Phillips Co. The electronic control unit and the quadrupole sensor are shown attached to the vacuum system in Fig. 1. This instrument has a mass range from 0 to 750 atomic mass units and will accomplish unit resolution up to 500 amu. Thus the toxic spacecraft contaminants of interest in this program lie within the working range of this spectrometer.

3. Environmental Sampling System

The gas inlet and sampling system shown in Fig. 10 was designed for direct analysis of gaseous environments over a wide range of pressures. Another feature of this design is the ability to utilize a high pressure in the ion source chamber while the mass spectrometer is under ultra-high vacuum (see Section 4 below for a detailed description). The ultimate advantage of this procedure is an overall increase in sensitivity since the ion source operates at high efficiency for the ions because the detector unit is free of interfering gas. The response of the spectrometer is also stable over a period of time and thus available for continuous or repeated comparisons of data.

4. Ultra-High Vacuum System

Two vacuum systems are employed with this mass spectrometer system. The first is a high throughput diffusion pump system attached directly to the ion source section. This pumping system permits the sampling of any gas, even inert species, since the diffusion pump is capable of handling all gases. A liquid nitrogen cooled chevron type baffle is used to block the backstreaming of hydrocarbons from the pump. Another precaution has been taken to protect the cleanliness of the ion source system; a large conductance valve has been located between the pumping system and the ion source chamber. Thus the chamber may be isolated from the diffusion pump during hold periods when the liquid nitrogen trap is not active. During these periods of time the chamber may be connected, via a second valve, to an ultra-high vacuum getter-ion and sublimation pumping system, see Fig. 7. The latter pumps provide continuous ultra-high evacuation of the mass spectrometer chamber. When the latter of the two valves, mentioned above, is closed the ion source chamber is essentially isolated from the ultra-high vacuum mass spectrometer chamber and opened via the first valve to the diffusion pump. Thus relatively high gas pressures and corrosive gases may be sampled without contamination of the mass spectrometer. This ability to differentially pump the ion source and detector stages permits continuous and unrestricted sampling of gaseous environments.

5. Mass Spectra - Results and Discussion

The results of this program to date have established the feasibility of utilizing a carbon filament as a field ion emitter source for mass spectrometry. The improvement in ion yield with this new design ion source should make this technique competitive with conventional electron bombardment mass

spectrometers.

The ion lens and energy retarding system are currently being perfected. Preliminary mass spectra, see Fig. 11, have been obtained with the complete field ionization mass spectrometer system. The mass spectrum shown in Fig. 11, although preliminary, does show that trace signals (10^{-16} amp) can be distinguished from the background. A recording system biased above the background level (indicated by the dashed line in Fig. 11) would respond to the two trace gas signals for mass numbers 18 and 28 as seen in Fig. 11.

Total ion yield measurements in the bulb will be continued in an effort to optimize operating conditions for maximum yield and correlate theoretical and experimental results.

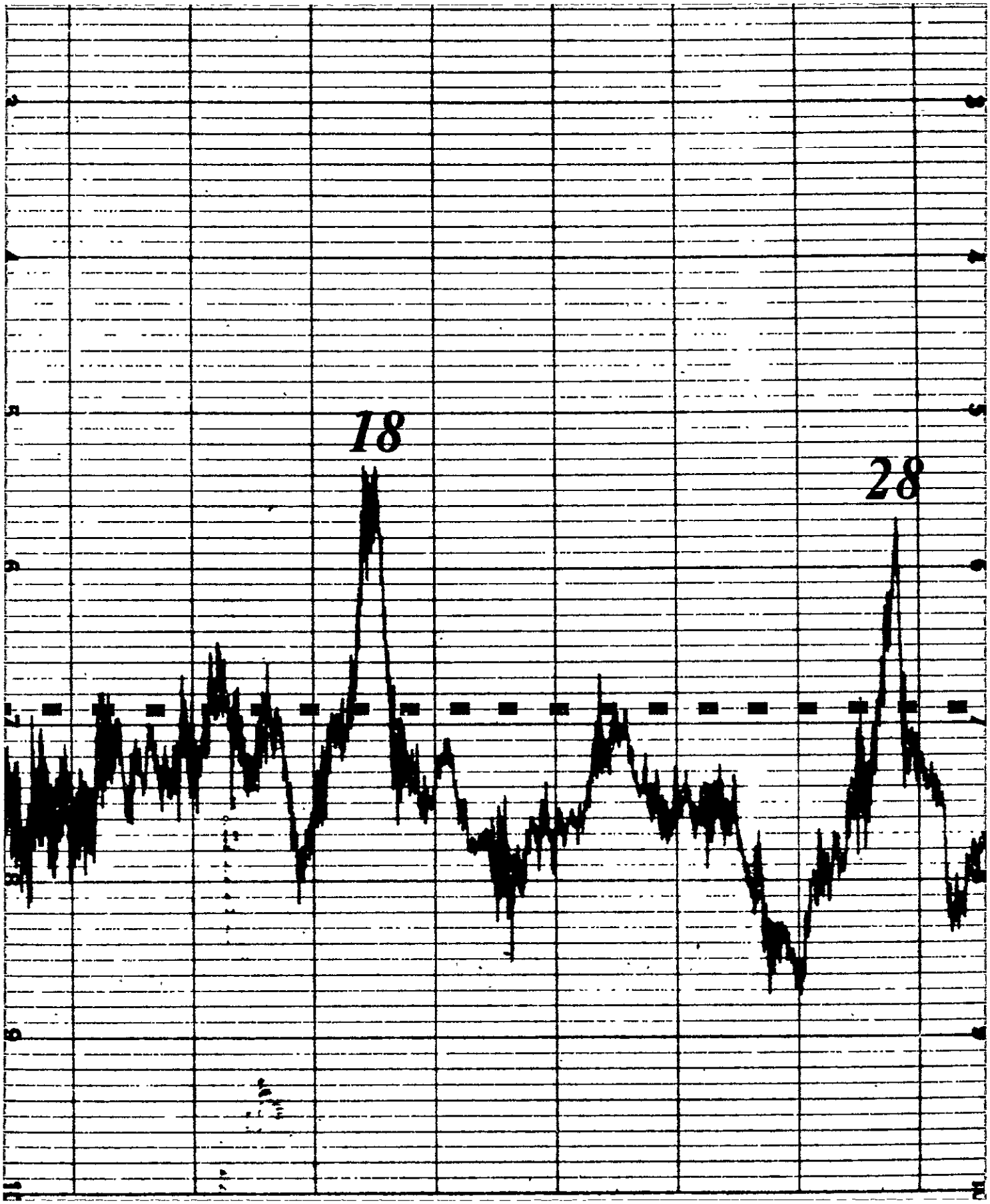

Fig. 11. Field Ion mass spectra showing trace gas signals for water vapor (18) and nitrogen (28) above the backbround level (dashed line).

APPENDIX I. Field Ionization Using a Cylindrical Emitter

The physical process involved in the generation of ion current by field ionization is a complex interaction of several variables. The primary variables treated here are: electric field, emitter geometry, emitter and gas temperatures, emitter material, and the specific gas molecules being ionized.

At high field strengths all of the molecules arriving at the emitter are ionized. The ion current, for the high field case, is therefore just the ionic charge times the number of molecules arriving at the emitter. The number of molecules attracted to the emitter is given by the supply function Z which exceeds the normal number bombarding the geometric area of the emitter because neutral molecules are polarized and attracted to the emitter by the high field. At lower fields there are many other considerations. The high field case is important because higher fields produce greater ion currents and the supply function may be checked directly by experiment without recourse to transmission probabilities.

A. The Electric Field of a Cylindrical Emitter

Previous reports[6,7] have presented analyses of the electric field on the basis of tip emitters. Now we wish to consider an emitter with cylindrical geometry. The field will cause a polarization of the gas molecules and draw them toward the emitter and the region of high ionization probability. The emitter is considered to be a cylinder of length L and very small radius R_o with supports at each end. The surface of the emitter is considered to be a "smooth" cylindrical surface. The field is assumed to be that of an infinite conducting cylinder of radius R_o. The finite length of the cylinder and the end supports are ignored. The distances that are important in the capture of molecules are quite close to the emitter so end effects contribute little to the field over most of the emitting surface. In addition, the supports will not have sufficient field strength to contribute to the supply of molecules. Effects due to image forces are not considered in the field contributing to the supply function because we are dealing with weakly interacting forces between the emitter and the polarized molecules. However, we cannot neglect these forces when dealing with the transmission probabilities of the electrons from the molecules to the emitter surface because there the image force is between the full charge of the electron and the surface.

The field of an infinite conducting cylinder is given by

$$F = \frac{\sigma}{\varepsilon}\left[\frac{R_o}{r}\right] \quad (1)$$

where σ is the charge in coulombs per unit area. If b is the radius of the accelerator (a concentric cylinder to the emitter) then at r = b the potential is equal to zero. At $r = R_o$ the potential is V_o yielding

$$\frac{\sigma}{\varepsilon_o} = \frac{V_o}{R_o \ln\left[\frac{b}{R_o}\right]} = F_o \; . \quad (2)$$

Previous work with metal tips was concerned with an image field (for field emission) and the compression factor due to the shank effects upon the tip end. These items are not considered important for cylindrical emitters, for the reasons described above.

B. The Supply Function of Gas Molecules to a Cylindrical Emitter

The potential energy for a particle in a field F is

$$-V(F) = P_d F + \tfrac{1}{2}\alpha F^2 \quad (3)$$

where α is the polarizability of the gas molecules and P_d is the permanent dipole moment.

Since the field is a function of r only for this central force problem, the angular momentum is conserved. Such a problem can be treated as one-dimensional with the centripetal force taken into account. This is done by forming an effective potential. The expression for total energy is

$$E = T + V = kT = \tfrac{1}{2} m\dot{r}^2 + \tfrac{1}{2} mr^2\dot{\phi}^2 + V(r) \quad (4)$$

The angular momentum is

$$L = mr^2\dot{\phi} \; .$$

The effective potential becomes

$$V_{eff}(r) = V(r) + \frac{L^2}{2mr^2} \quad (5)$$

The angular momentum can be expressed as

$$L = mvr'$$

where r' is the distance of closest approach if the field were zero. The term v is given by

$$v = v_{rms} = \sqrt{\frac{2kT}{m}} \qquad (6)$$

where the factor 2 is due to the cylindrical geometry which has two dimensions of escape, while the spherical geometry has three. The angular momentum is now

$$(2mkT)^{\frac{1}{2}}r' \qquad (7)$$

Substituting for L in Eq. 5 we have

$$V_{eff} = V(r) + kT\left(\frac{r'}{r}\right)^2 \qquad (8)$$

The centripetal velocity is $-\frac{dr}{dt}$, thus from Eq. 4 we have

$$-\dot{r} = \sqrt{\frac{2}{m}}\left(E - V_{eff}\right)^{\frac{1}{2}} .$$

For impingement, $\dot{r}$ must be real at R_o, and for grazing incidence at $r = R_o$,

$$E - V_{eff} = 0 \quad .$$

For cylindrical geometry a Z-component of velocity cannot aid the escape of a gas molecule from the electric field. Thus the Z-component of energy $E_3 = 3/2$ kT will be taken to be $E_2 = kT$ since E_3 is parallel to the long cylinder axis. We may write

$$\left(\frac{r'}{R_o}\right)^2 = 1 - \frac{V(r')}{kT} = \sigma_c \qquad (9)$$

noting that $-V(r)$ is positive. The effective cross-sectional area of capture is $2\pi rL$ where L is the length of the cylindrical emitter. The supply function for the cylindrical emitter is

$$Z = 2\pi R_o \sigma_c^{\frac{1}{2}} L \quad . \qquad (10)$$

If the ionic charge is q and the number of molecules hitting a unit cross-section of area per unit time is $p(2\pi mkT)^{-\frac{1}{2}}$, then the ion current for a sufficiently high field is

$$i = qZ = q2\pi R_o \sigma_c^{\frac{1}{2}} L p(2\pi mkT)^{-\frac{1}{2}} \qquad (11)$$

where p is the gas pressure. This Expression (11) is subject to the condition that the field is high enough to ionize all molecules captured before they reach the cut-off distance X_c. Ionization cannot take place for any molecule that is closer than X_c to the emitter surface because of the filled states below the Fermi level of the emitter material.

The differences between the low and high field cases are illustrated in Fig. 2 which shows the number of molecules N(X) ionized at a distance X from the surface. The critical distance X_c is indicated.

In the low field case the ionization rate is small compared to the rate of arrival of the gas molecules. The ion current in this case is the equilibrium concentration of gas molecules near the tip divided by the mean life time of the ionization of these molecules.

The equilibrium concentration near the tip differs from the concentration of the gas because of the possible temperature difference and the attraction of the polarized molecules in the high field near the emitter. The tip concentration can be written as

$$C_t = C_g f(T_g/T_t) e^{-V(F)/kT_g} \qquad (12)$$

The function $f(T_g/T_t)$ is dependent upon the kinetic mechanism. The Boltzmann factor of the field potential is analogous to the atmospheric barometer relationship. The function $f(T_g/T_t)$ is is unity at a distance slightly in excess of the average hopping height, the temperatures are nearly equal at this height.

Consider a surface at temperature T_t and a gas at temperature T_g. An equilibrium condition is reached, we now seek the zero field equilibrium concentration at the surface. Let there be an artificial barrier through which an equal number of molecules pass traveling each way. The flux ϕ across the barrier is expressed as

$$\Phi_{in} - \Phi_{out} = 0$$

and assuming an ideal gas

$$\frac{P_g}{\sqrt{2\pi mkT_g}} = \frac{P_t}{\sqrt{2\pi mkT_t}}$$

with

$$p = CkT.$$

We have

$$C_t = C_g\left(\frac{T_g}{T_t}\right)^{\frac{1}{2}} \exp[-V(F)/kT_g]$$

by adding the effect of the field.

If full thermal accommodation takes place this relationship should hold in the region where most of the ionization takes place for our low field restriction. If the concentration near the emitter is truly an equilibrium concentration, the ion current generated in a volume element about the cylindrical surface is

$$di = qC_t\tau^{-1}dV$$

with $dV = 2\pi rLdr$ and with τ the lifetime of an electron in its bound state. The calculation of τ is the major part of the problem and much attention is given to it later.

We define τ as

$$\tau = (\nu_e D)^{-1} \tag{13}$$

where ν_e is the arrival rate of the electron to the barrier and D is the tunneling probability.

For the low field case the total ion current is

$$i = 2\pi LC_g q\tau^{-1}\int_{R_o}^{\infty} r\, f\left(\frac{T_g}{T_t}\right)\exp[-V(r)/kT_g]dr$$

Letting all functions be at the value they have at R_o, as a low field assumption, the ion current becomes

$$i \simeq 2\pi LC_g\tau^{-1}qR_o\left(\frac{T_g}{T_t}\right)^{\frac{1}{2}}\exp[-V(F_o)/kT_g\int_{R_o}^{R_o+X_c}dr$$

$$i \simeq 2\pi L C_g \tau^{-1} q R_o \left(\frac{T_g}{T_t}\right)^{\frac{1}{2}} \exp[-V(F_o)/kT_t] X_c \qquad (14)$$

It is logical to ask at this point the value of taking data at such a low field; some reasons are listed below:

1) The surface uniformity, i.e. the percent of the surface that is actually emitting, when compared to the high field case, may be determined;

2) A measurement when a retarding potential is used of the theoretical X is possible;

3) The presence of liquid layer may be estimated for various emitter temperatures.

The field strength is high enough in the intermediate field case to decrease the steady state concentration near the emitter, yet not sufficient to ionize all of the captured molecules before they reach the critical distance X_c. Thus kinetic considerations must be used in computing the ion current for intermediate field values. Multiple rebounds of molecules from the emitter surface with the thermal accommodation of each bounce must also be considered.[6,7] Thus, detailed theories of thermal accommodation[8,9,10] must be used to predict quantitative values of ion current for the intermediate field case.

APPENDIX II. Calculation of Transmission Probabilities

The problem of calculating ion yield currents from a field emitter can be divided into two parts: the calculation of the supply of gas molecules, and the ionization rate. The supply of the gas molecules to the emitting surface is a problem of gas kinetics and geometry. The ionization rate involves the basic quantum mechanical mechanism of the field ion process.

This report is primarily concerned with the latter problem of ionization rate. The ion current from a cylindrical emitter for low field approximations is

$$i \simeq 2\pi L C_g \tau^{-1} q R_o \left(T_g/T_t\right)^{\frac{1}{2}} \exp[-V(F_o)/kT_g] X_c$$

where L is the length of the cylinder, C_g is the concentration of gas, τ is the life time of the ionization process, q is the electronic charge, R_o is the radius of the cylinder, T_g is the gas temperature, T_t is the temperature of the emitter, $V(F_o)$ is the potential about the emitter, the electric field is F_o, and X_c is the critical ionization distance. We define τ as

$$\tau = [\nu_e T\left(E_d\right)]^{-1}$$

where ν_e is the arrival rate of the electron to the barrier and $T\ E_d$ is the tunneling probability.

For the case of a high electric field[3] the ion current is given by

$$i = q 2\pi R_o \sigma_c^{\frac{1}{2}} L p (2\pi m k T)^{-\frac{1}{2}}$$

where

$$\sigma_c = 1 - V_o/kT_g \ .$$

The remaining problem is the solution for the quantum mechanical transmission probability. This problem was posed in the first report. We restate the problem here with the newly obtained computer calculations. The ionization probability D is at the heart of this field ionization problem. The original linear WKB approach has been applied to the problem with many improvements[6,7,11] as described below.

The condition for the application of the WKB method is

$$[\tfrac{1}{2}\pi](d\lambda/dx) << 1$$

where $d\lambda/dx$ is the spacial derivative of the de Broglie wave length. The above condition is often violated in field ionization problems. However, depending on the barrier shape, the WKB method can be valid for a much wider class of problems than the above condition allows[12]

Several three dimensional improvements to the calculation of field ionization transmission probabilities have been given using collision theory[13], variational methods[14], and perturbation theory[15]. The results predicted the half-width of the peak representing the ion energy spectrum.

Refinements of the image potential have been given[16] as it applies to the reflection and transmission of electrons through surface barriers. Many of these refinements apply to a conceptually similar problem in the periodic deviations from the Schottky line.

The basic understanding of the interaction between gas atoms and metal atoms of the tip in the presence of a high electric field took a different turn when structure was observed in the energy spectrum of the ions[18,19,3]. This structure had not been predicted by the quasi-classical WKB approximation. Calculations of this structure have been undertaken with the following interpretations: the effect arises from the fact that the surface potential is resonant to the energy of electrons entering the metal[3]; and the energy spectrum is due to the inference between waves reflected from the rapid variations in the atomic potential of the ionizing atom and the waves reflected from the rapid change in the potential at the metal surface[17]

The above interpretations of the structure in the energy spectrum are, in many ways, quite similar. Conceptual differences do exist however. These differences in interpretation appear to be related in a quantum mechanical sense to the Gamow and Fermi theories of alpha decay tunneling. In the former theory the tunneling particle was considered as a traveling wave transmitted and reflected from a potential barrier while the latter theory considered the particle to be initially in a bound state and then tunneling to a free state.

The experimental portion of this program is concerned with the improvement of ion current yield. Therefore a correlation will be sought with the theory which gives the best yield and peak half-width values rather than the best description of the structure refinement.

1. Transmission Probability Calculations by the WKB Method

Comparative calculations have been done to place the various theories into the same format. The linear WKB method[6,11] has been programed for a numerical calculation with a variety of conditions. The potential function of Fig. 3 is

$$V(x) = -\frac{e}{|\ell - x|} + Fx - \frac{e}{4X} + \frac{e}{\ell + x}$$

where x is the distance from the surface to the electron, a is the radius, and d is the distance to the ion center. The transmission probability is given by

$$D(\ell) = \exp\left[-\frac{(8em)^{\frac{1}{2}}}{\hbar}\int_{x_2}^{x_1}\{V(x) - Fd + V_I - \frac{e^{\frac{1}{2}}}{4d}\}dx\right]$$

The results of this calculation are given in Fig. 4 and Table II. The calculations were performed on the University of Missouri-Kansas City IBM 360 Computer using the Newton-Raphson method to find the integration limits and Simpson's rule for the integration. In order that these values may be compared with the other methods we have chosen the energy deficit parameter for comparison

$$E_d = \Theta + \mu_m + Fd - V_1 + e/4d$$

where $\Theta = 4.5$ eV, $\mu_m = 6.4$ eV, $F = 2.5$ eV/Å, $V_I = 15.6$ eV, and e is the electronic charge. These conditions are intended to simulate an experiment with H_2 as the gas and tungsten as the emitter metal. The peak half width (1 eV) is in agreement with Tsong and Müller's[11] calculated value which is twice their experimental value. Boudreaux[15] using a different potential value and calculation method on the one dimensional problem obtained a value four times the experimental value. These authors do not give absolute magnitudes for the transmission probability. Jason[3] does give a comparable result, however there seems to be some question regarding the units used. In general the WKB calculation is consistent with the usual difficulties, namely the half width is twice too wide, no fine structure is observed,[11,14,3] and the magnitudes are far too great.

B. The Direct Solution of the Linear Schrödinger Equation

A computer program for the calculation of transmission probabilities has been written and its limits verified. The range of values necessary for directly solving the linear

Schrödinger equation has been used for a potential barrier problem. Expressions for the transmission probabilities for the barrier in Fig. 5 have been obtained by solving

$$\frac{d^2\Psi}{d\xi^2} - \xi\Psi = 0$$

with

$$\xi = [x - (E - \phi - \mu_m)/F]\left(\frac{2mF}{\hbar^2}\right)^{1/3}$$

We have derived the following relationship for the transmission probability, which agrees exactly with Alferieff and Duke[17]

$$T(E_d) = \frac{4k_F^2}{\pi^2 k_L^2} \frac{1}{P^2 + Q^2},$$

where

$$P = [Bi(\xi_d)Ai(\xi_o) - Bi(\xi_o)Ai(\xi_d)] + \frac{k_F^2}{k_L k_R}[Bi'(\xi_d)Ai'(\xi_o) - Bi'(\xi_o)Ai'(\xi_d)],$$

and

$$Q = \frac{k_F}{k_R}[Bi'(\xi_d)Ai(\xi_o) - Ai'(\xi_d)Bi(\xi_o)] + \frac{k_F}{k_L}[Bi'(\xi_o)Ai(\xi_d) - Ai'(\xi_o)Bi(\xi_d)] .$$

where Ai(x) and Bi(x) represent the Airy functions, and the prime indicates the derivative with respect to the argument, with

$$k_F = (2mF/\hbar^2)^{1/3},$$

$$k_L = \sqrt{2mE_d/\hbar} ,$$

$$k_R = \sqrt{2m\left[E_d - V_R\right]/\hbar} ,$$

$$V_R = \phi + \mu_m + F_d - 2V_I \quad ,$$

$$\xi_o = - k_F(E_d - \phi - \mu_m)/F \quad ,$$

and

$$\xi_d = k_F[d - (E_d - \phi - \mu_m)/F] \quad .$$

The same parameters were chosen as in the WKB calculation for the purpose of comparison. These results are given in Fig. 6 and Table III.

The results obtained by this calculation are in complete agreement with Alferieff and Duke.[17] The fine structure peaks are positioned near those predicted by the triangular well calculation.[18] This calculation predicts values some four orders of magnitude less than the WKB method.

The calculations described above will be applied to the experimental program. A value of life time (τ) will be calculated from the various experimental parameters. In the low field case the height of the main peak at the critical distance $T(E_{dc})$ will give the lifetime. This lifetime with the known supply function permits a calculation of the ion yield. These example calculations illustrate the workability of the method. The computer programs are available and working. Only the proper data cards need be inserted for the calculations relationship to the experimental part of the program.

In order to predict the effects of increasing field strength on the magnitude of the transmission probability, a calculation was performed using the direct solution of the Schrodinger equation with a varying field strength. These results are given in Fig. 7 and Table IV. In the range of practical experiments there is an increase of two orders of magnitude in the transmission probability for each additional increase in field strength of one volt per angstrom. An increase of the supply function would increase the ion yield even further.

The calculations reported above have all been carried out in one dimension. Three dimensional corrections can be used to approximate the real situation when required by the conditions. This correction can be done by calculating the

ionization probability for each θ, neglecting the angular Laplacian, then evaluating the integral of the weighted probability

$$\frac{1}{\tau} = \frac{1}{2}\int_0^{\pi} \frac{\sin\theta}{\tau(\theta)} d\theta$$

for the total lifetime. The above correction is only necessary for the intermediate field case and will not be used for low field calculations.

APPENDIX III. Improvements to Field Ionization Theory

A new theoretical description of the field ionization process is now being developed as outlined below. The results and predictions obtained should give a better understanding of the practical applications of field ionization.

A. Molecular Orbital Characterization of an Emitter Surface

A great number of improvements have been offered in the theory of the field ionization process and further refinements would likely prove to be unobservable in the experimental data. It is striking to notice that all of the computational models used to date have characterized the emitter material by a work function and a Fermi level only. Recently published experiments[20] are interpreted to suggest that this characterization may not be sufficient. Greater brightness in the field ion microscope images of certain crystal planes of the emitter suggest that the atomic orbitals that are intersected by the surface plane accept electrons from the molecules being ionized. The planes which have more orbitals protruding ionized more efficiently. In the perspective of this model, "field ion images are interpreted as projections of regions where the fully occupied orbitals of inert image gas atoms can easily overlap with the partially occupied single or hybridized orbitals of the surface atoms of the emitter."[20] These surface atoms are viewed as preserving, to some extent, their individual character. The wave functions of the surface atoms approximate the wave function the same as the isolated atom would have. This view is taken by many in the study of chemisorption and catalysis. More support for this model is inferred in current theories on hydrogen promotion of field ionization and rearrangement of surface charge.[21]

The unique feature of the experimental phase of the program is the cylindrical emitter of large area and smooth surface. It would seem natural to use this feature of the emitter to study the surface of graphite and improve the theory from that direction rather than to concentrate on the field and gas molecule side of the problem.

1. Localized Wave Functions - Delocalized Wave Functions

Caution must be exercised in considering the molecular orbital model of the surface. The electronic configuration of a metal-adsorbate system in a high electrid field has been treated by self-consistent calculations[22] where the possibility of localized surface states are ignored.

It is felt that in the field ionization problem the separation distance between the gas molecule and the emitter surface is sufficiently great so that the proper description lies somewhere in between the totally localized and the totally delocalized picture of the electronic wave functions.

2. The Use of Time Dependent Perturbation Theory in Computing Transition Probabilities

The approach to computing the transition probability of an electron from the gas molecule to the emitter surface should be attempted by the use of time dependent perturbation theory.[23,15]

When the gas molecule is near the emitter surface, the electron is subject to perturbations by the surface forces and the external field which can induce a transition of the electron into the emitter. Letting V be the potential energy of all such forces, the probability per unit time of such a transition can be calculated using the well-known result

$$P = \left(\frac{2\pi}{h}\right) g(E_e) |\langle \Phi_e | V | u_o \rangle|^2$$

where Φ_e is the protuding molecular orbital of the emitter surface, u_o is the ground state wave function of the gas molecule, and $g(E_e)$ is the density of states.

The transition time is given by

$$t(\ell) = \frac{1}{P} \quad .$$

The probability of being ionized in the distance ℓ to $\ell + d$ is

$$P(\ell)d\ell = \frac{dt}{t(\ell)} = \frac{d\ell}{vt(\ell)}$$

where v is the radial component of the velocity of the molecule about the emitter. The probability of being ionized on one pass is

$$P_{total} = \int_{X_c}^{\infty} P(\ell)d\ell$$

For a smooth graphite surface the carbon atoms are found in the usual hexagonal arrangement with hybridized $(sp)^2$ orbitals forming the sigma bonds between them. The unhybridized partially filled p_z orbitals are perpendicular to the surface forming the pi cloud that rings each hexagon. In this approach it is assumed that the transition of the electron of the gas molecule will be into this pi cloud.

This orbital view calls for a reinterpretation of many of the parameters of the field ionization process, notably the critical distance x_c. A possible inclusion of the band structure of the emitter material, graphite,[24] may be necessary.

B. Band Theory and Field Ionization

The essential physical process of field ionization has had several different descriptions.[3,6,7,13-18] Improvements to field ion theory have been in two major categories, refinements in the potential of the electric field and in molecule combination and methods of calculating transmission probabilities. Previous theories of field ionization have assumed a free-electron model for the metallic emitter. The purpose of the present effort is to consider the metal to be a system of periodic potentials (see Fig. 12). In such a system, the electrons are described by Bloch wave functions and the values of real energy are characterized by a series of bands (see Fig. 13).

The need for a more rigorous theory is indicated by recent experimental facts. Knor and Müller[20] observed regional brightness in the field ion microscopy patterns. Different crystal faces have shown different ionization efficiencies. These results indicate that the periodic nature of the metallic crystal is an important consideration. An energy analysis of the ion beam by Jason[3] has shown the onset peak to consist of double peaks whose relative heights are voltage dependent. Peak height and resolution are observed to vary with crystal orientation.

Surface states (Tamm states)[25,26] result from the termination of the periodic system at the metal interface. These states are dependent upon crystal direction. They provide energy states for the reception of electrons from the gas phase molecules. The transition of electrons from the bound state of the molecule to the Bloch bands of the crystal is probably closer to describing the essential physical process than any of the previous theories.

C. One-Dimensional Brillouin Zones

The understanding of a complex quantum mechanical process can be best achieved through a one-dimensional model. Once the basic formulation is obtained, the extension to directional features can be straight forward. An outline of the one-dimensional formulation is given in this section.

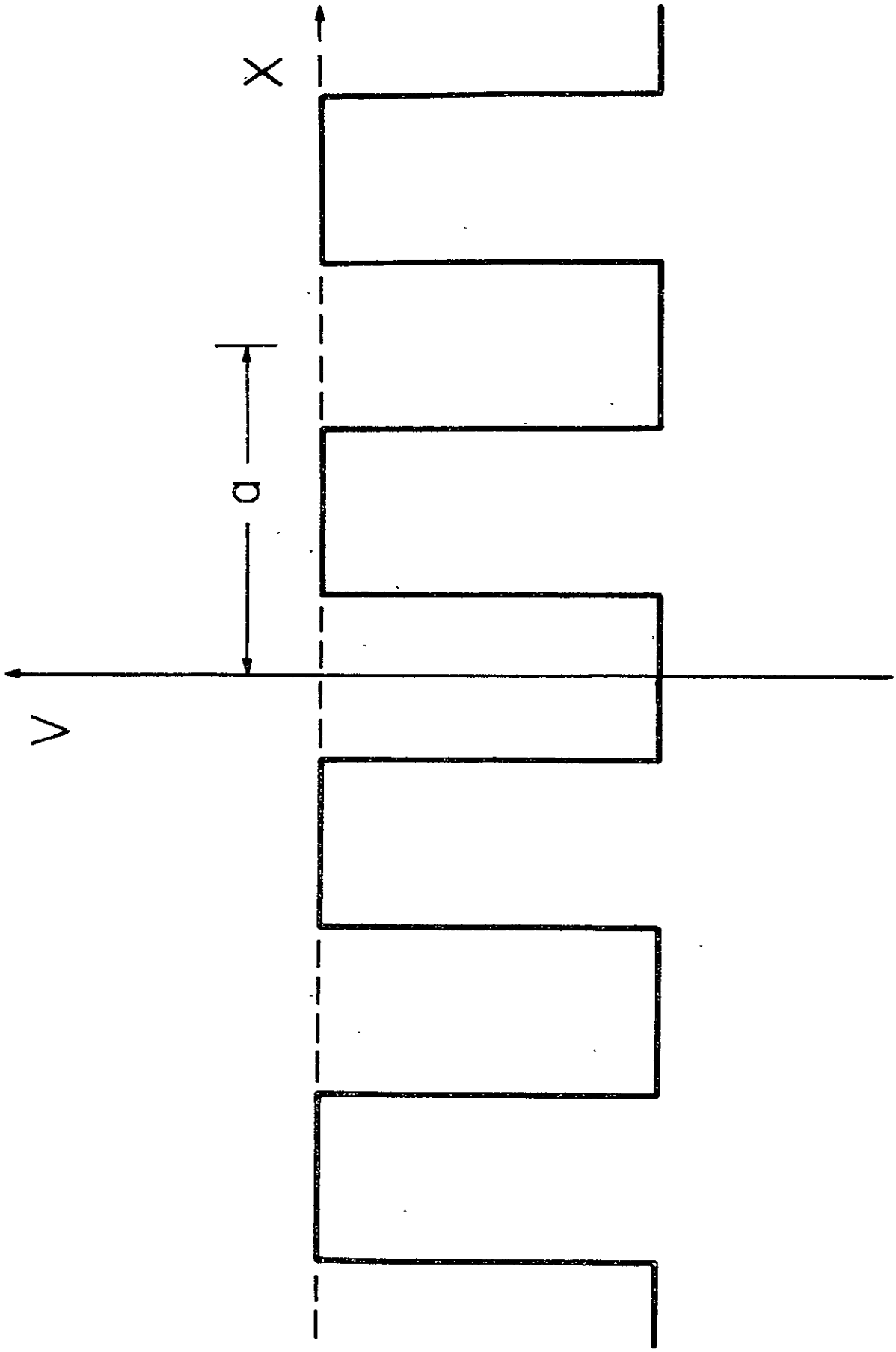

Fig. 12. Periodic potential in one dimension.

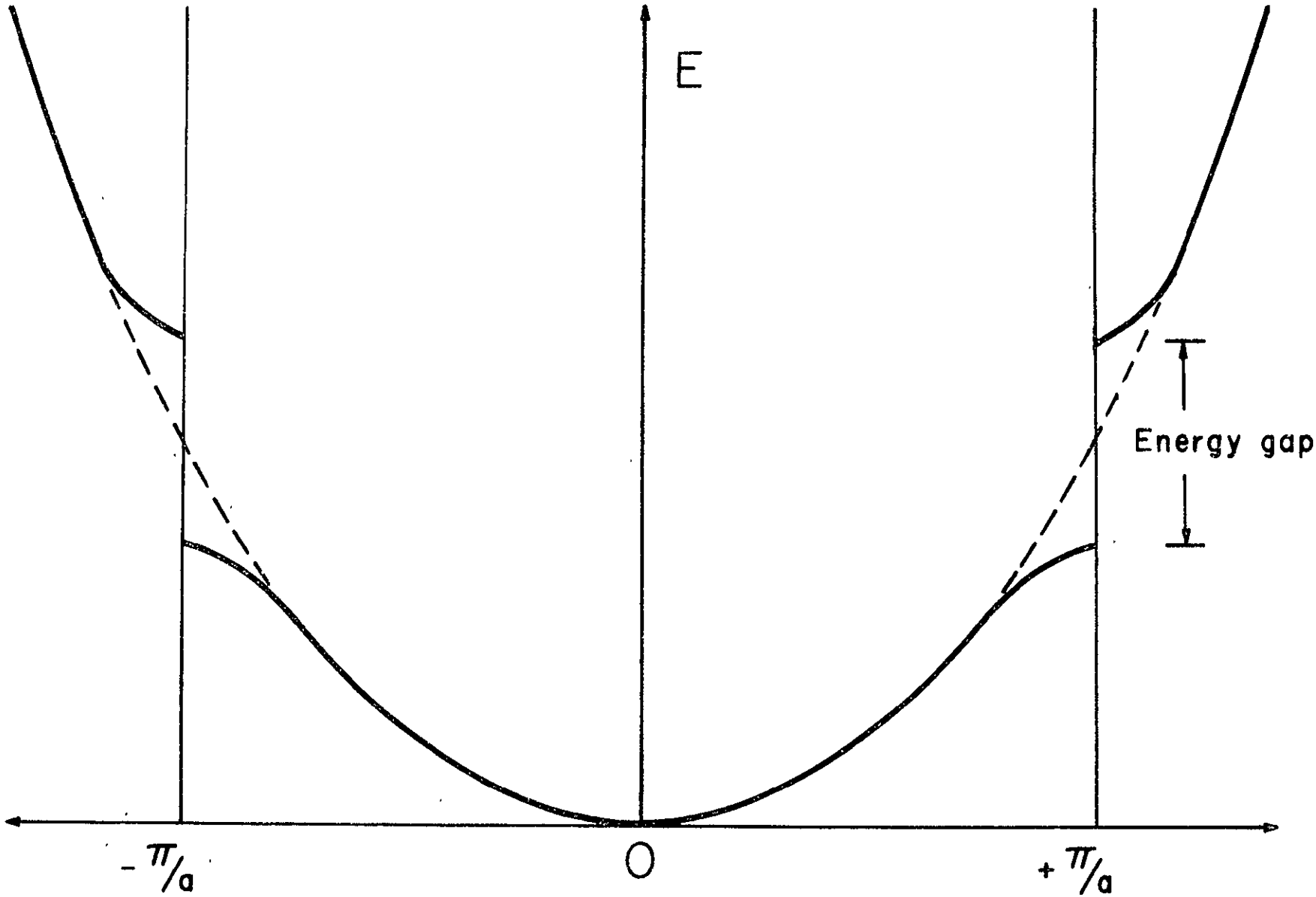

Fig. 13. Energy as a function of wave number for electrons in a one-dimensional periodic potential.

The motion of an electron in a one-dimensional lattice is described by the Schrödinger equation with a periodic potential (see Fig. 12). We may write it as

$$[- d^2/dx^2 + V(x)] \psi(x) = E\psi(x) \qquad (5)$$

where

$$V(x + a) = V(x) \quad .$$

The Bloch wave solutions for the allowed values of real E are of the form

$$\psi_{n,k}(x) = u_{n,k}(x)e^{ikx}, \; n = 0, 1, 2, \ldots \qquad (6)$$

where $u_{n,k}(x)$ has the same periodicity as V(x) and k is taken as real. The corresponding eigen values are the energy bands,

$$E = E_{n,k}, \; n = 0, 1, 2, \ldots \qquad (7)$$

The energy bands are separated by forbidden ranges of E (see Fig. 13) in which wave functions are of the form of Eq. (6), but with k as a complex variable

$$k = k_r + ik_i \quad .$$

When E lies in a band gap there are still two solutions for ψ in the periodic potential. An ordinary second order differential equation must always have two solutions. These solutions are evanescent waves, one increasing and the other decreasing on the average exponentially with x. In Particular, we have

$$\psi_{\pm}(x+a) = - \exp(\pm k_i a)\Psi_{\pm}(x)$$

for the band gap at $k = \pi/a$.

E may be defined for complex k. Tee energy E is, in general, complex but it is real along the real axis and at values of k of the form

$$k = (\pi/a) \pm ik_i$$

(See Figs. 14 and 15). On the path of real E one may pass continuously from one energy band to another.

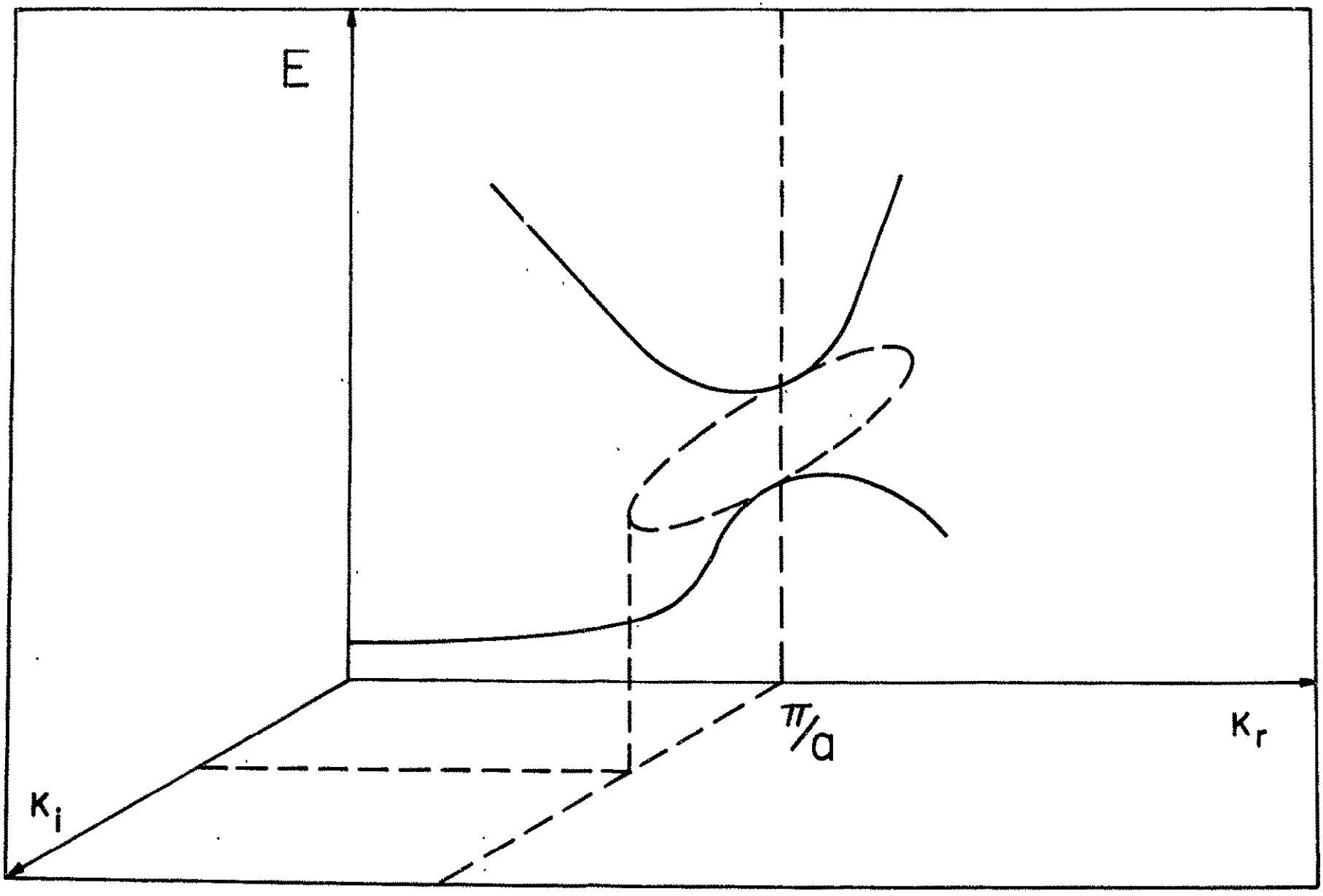

Fig. 14. Lines of real E in complex k space.

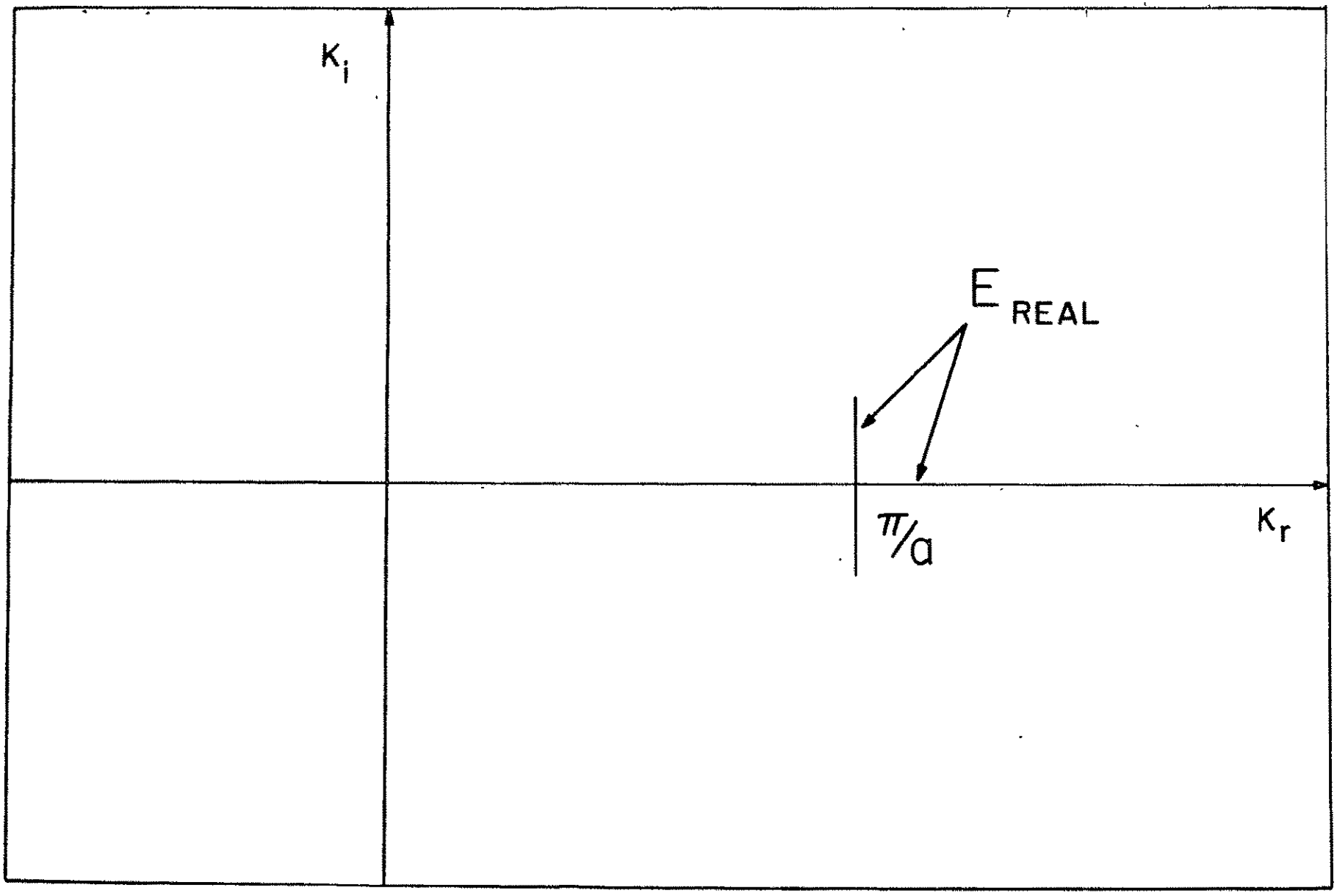

Fig. 15. Regions in complex k space where E is real

In consideration of the bulk properties of metals, both exponential wave functions are ignored because the increasing wave function is not normalized and the decreasing wave function does not extend far enough from an individual lattice site to contribute to bulk effects. The exponential tails of the metal wave functions are important, (see Fig. 16). At an interface or free surface the expontential tails are the extensions of the metal wave functions into the vacuum. Since, the exponential tails are extensions of the metal wave functions they depend upon the k-vector direction, i.e. they vary in length depending on the crystal direction of the interface. This directional dependence is the element needed to explain, hopefully, the recent experimental results.[7,12]

Fundamentally, the problem is one of matching the wave function of the crystal to the wave function outside the surface. In the case of field ionization the potential outside the surface is further complicated by the presence of gas molecules and a high electric field (see Fig. 17). The wave function for the free side of the surface, is for an electron of energy E, determined by the field strength and the distance of the gas molecule from the metal surface. In the electric field the wave function is in terms of Airy functions with E the independent variable. The free electron wave function is them matched to the appropriate energy Bloch wave function in the metal.

E and ψ can be derived, for complex k, from what is known regarding the ordinary band states at real k. In fact, the whole modern apparatus of orthogonalized plane waves and pseudo-potentials for calculating band structures can be applied to determining the evanescent waves. With the evanescent waves determined for the periodic crystal, the matching problem of the ψ_L (the crystal wave function to the ψ_R (the free particle wave function) can be carried out. There is only one constant to adjust; therefore, the match is made for a particular E. Plotting ψ'/ψ for ψ_R and ψ_L over a range of E, an intersection can occur thereby determining the allowed surface state (see Fig. 18).

The wave function inside the crystal is determined by the energy band structure with evanescent solutions of the Schrödinger equation. The wave function outside is a sum of incident and reflected electron waves. The correct combination of these is determined by the matching calculation. Electrons incident on a crystal surface are partly transmitted to states of the same energy inside the crystal and partly reflected to states of the same energy outside. The knowledge of the correct combination would give the ionization

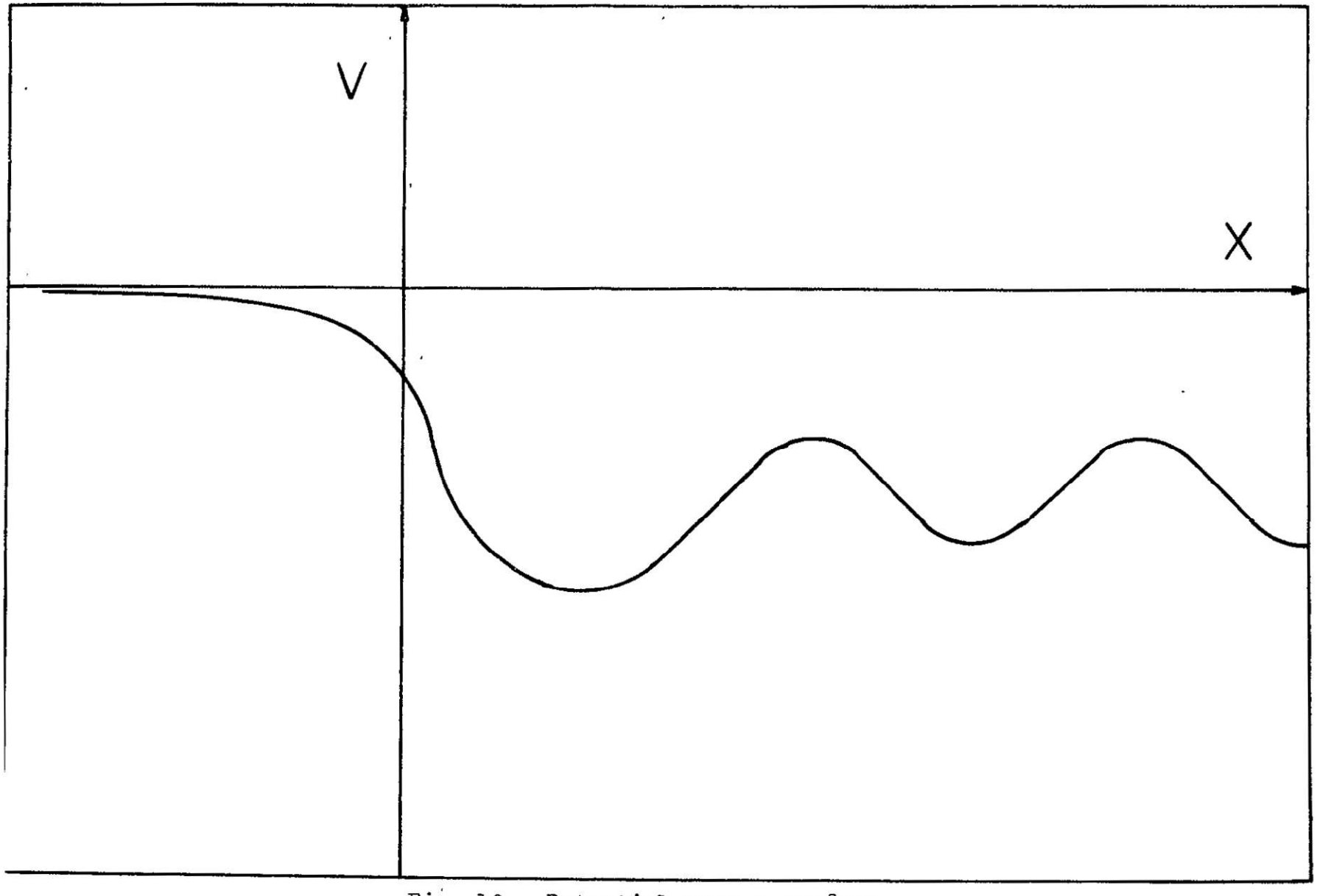

Fig. 16. Potential near a surface.

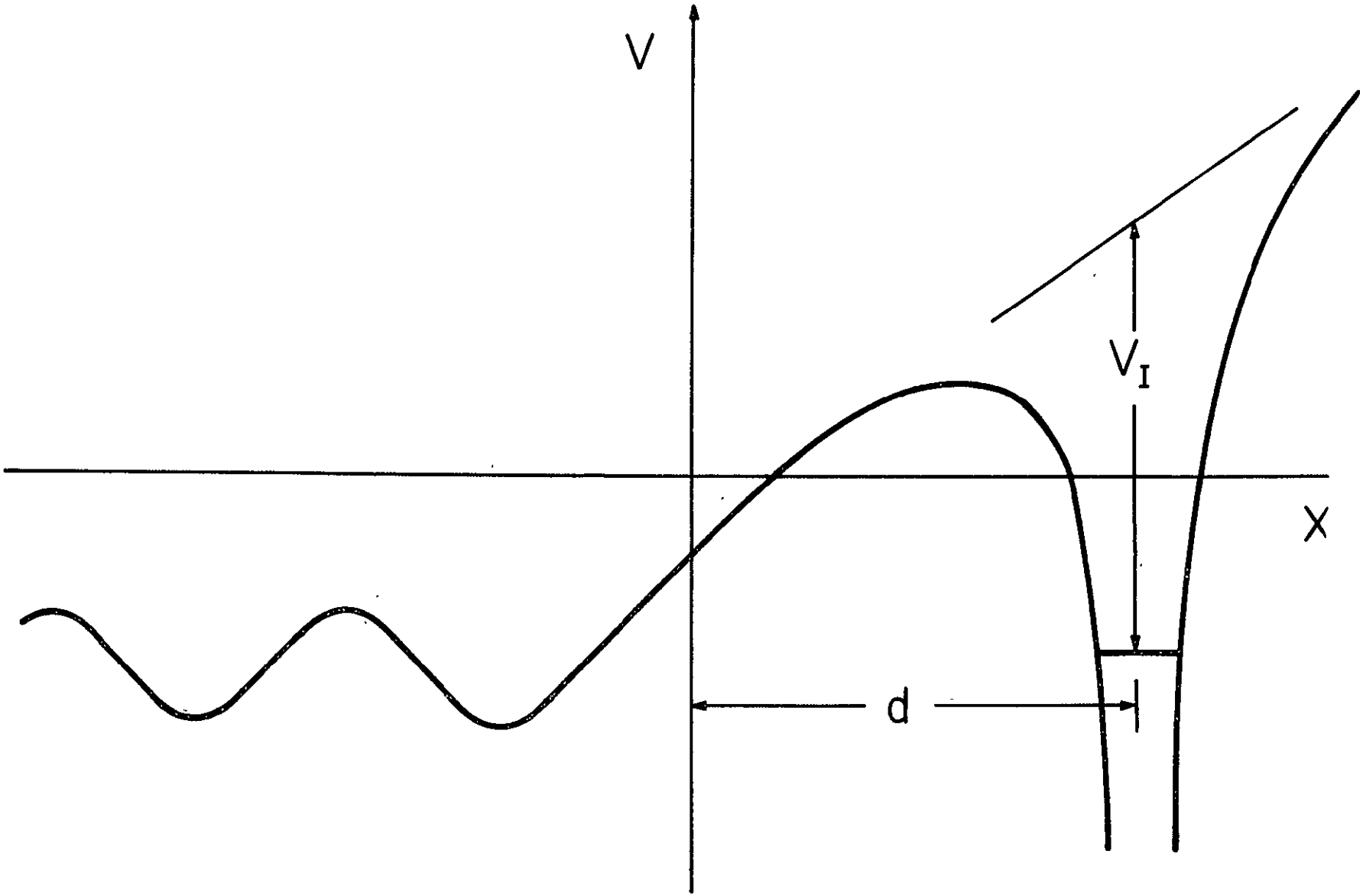

Fig. 17. Potential near a surface of a molecule in an electric field.

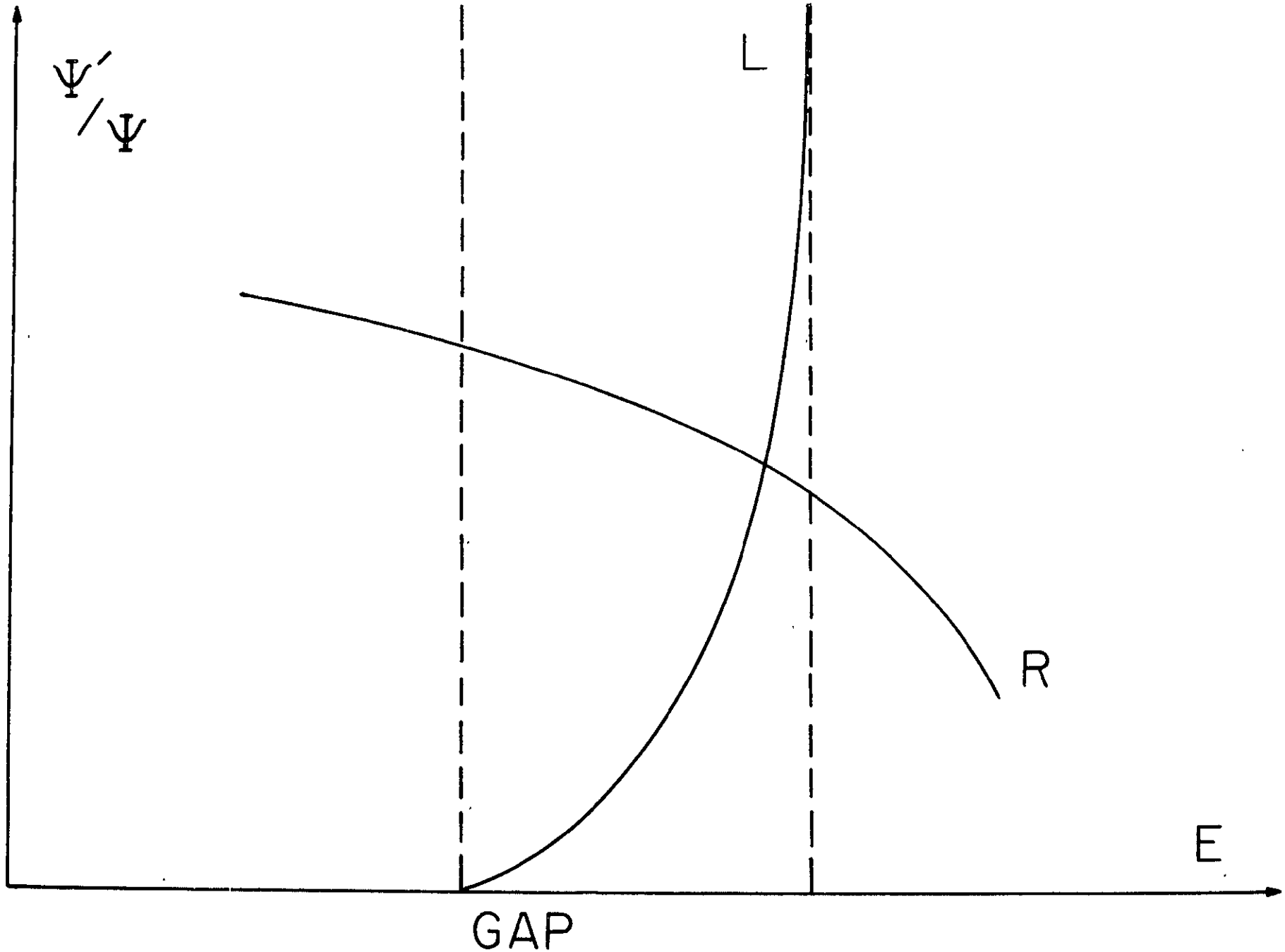

Fig. 18. Matching Ψ′/Ψ at a surface.

efficiency. Thus, this new theoretical description of the field ionization process should yield data to predict the practical applications of field ionization.

REFERENCES

1. A. J. B. Robertson and B. W. Viney, Brit. J. Appl. Phys. 14, 278 (1963).

2. H. D. Beckey, Et Al, J. Sci. Instr., 1, 118 (1968).

3. A. J. Jason, Phys. Rev., 156, 266 (1967).

4. H. A. Enge, Rev. Sci. Instr., 30, 248 (1959)

5. V. K. Zworykin, Et Al, Electron Optics and the Electron Microscope, (Wiley, New York, 1945) Chapter 13.

6. E. W. Müller, Advances in Electronics and Electron Physics 13, (Academic Press, New York, 1960) P.83.

7. R. Gomer, Field Emission and Field Ionization (Harvard University Press, Cambridge, Massachusetts, 1961).

8. R. E. Harris, J. Chem. Phys. 46, 3217 (1967).

9. F. O. Goodman and H. Y. Wachman, J. Chem. Phys. 46, 2376 (1967).

10. L. M. Raff, J. Lorenzen, and B. C. McCoy, J. Chem Phys. 46, 4265 (1967).

11. T. Tsong and E. Q. Müller, J. Chem. Phys. 41, 3279 (1964).

12. W. D. Getty, Report on the 26th Annual Conference on Physical Electronics, 375.

13. D. S. Boudreaux and P. H. Cutler, Phys. Rev. 149, 170 (1966).

14. D. S. Boudreaux and P. H. Cutler, Solid State Comm. 3, 219 (1965).

15. D. S. Boudreaux and P. H. Cutler, Surface Science 5, 230 (1966).

16. P. H. Cutter and J. C. Davis, Surface Sci. 1, 194 (1964).

References (cont.)

17. M. E. Alferieff and C. B. Duke, J. Chem. Phys. 46, 938 (1967).

18. A. J. Jason, et al, J. Chemical Phys. 43, 3762 (1965).

19. A. J. Jason, et al, J. Chem. Phys. 44, 4351 (1966).

20. Z. Knor and E. W. Müller, Surface Sci. 10, 21 (1968).

21. E. W. Müller, Surface Sci. 8, 462 (1967).

22. A. J. Bennett and L. M. Falicov, Phys. Rev. 151, 512 (1966).

23. S. Raimes, The Wave Mechanics of Electrons in Metals (Amsterdam, North Holland Publishing Co., 1961).

24. J. C. Slonczski and P. R. Weiss, Phys. Rev. 109, 272 (1958).

25. V. Henine, Proc. Phys. Soc. 81, 300 (1963).

26. V. Henine, Surface Sci. 2, 1 (1964).